Elsevier Editorial System(tm) for Neuropharmacology

Manuscript Draft

Manuscript Number:

Title: In-vivo effects of knocking-down metabotropic glutamate receptor 5 in the SOD1G93A mouse model of amyotrophic lateral sclerosis

Article Type: Research Paper

Keywords: Amyotrophic lateral sclerosis
SOD1G93A mouse model
Metabotropic glutamate receptor type 5
Metabotropic glutamate receptor type 5 knock down
Glutamate transmission
Clinical disease progression

Corresponding Author: Professor Giambattista Bonanno,

Corresponding Author's Institution: University of Genoa

First Author: Tiziana Bonifacino, PhD

Order of Authors: Tiziana Bonifacino, PhD; Luca Cattaneo, PhD; Elena Gallia, Dr.; Aldamaria Puliti, PhD; Marcello Melone, Prof.; Francesca Provenzano, Dr.; Simone Bossi, Dr.; Ilaria Musante, PhD; Cesare Usai, Prof.; Fiorenzo Conti, Prof.; Giambattista Bonanno; Marco Milanese, PhD

Abstract: Amyotrophic lateral sclerosis (ALS) is a fatal neurodegenerative disorder due to loss of upper and lower motor neurons (MNs). The mechanisms of neuronal death are largely unknown, thus prejudicing the successful pharmacological treatment. One major cause for MN degeneration in ALS is represented by glutamate(Glu)-mediated excitotoxicity. Activation of Group I metabotropic Glu receptors (mGluR1 and mGluR5) at glutamatergic spinal cord nerve terminals has been reported to produce abnormal Glu release in the widely studied SOD1G93A mouse model of ALS. We also reported that halving mGluR1 expression in the SOD1G93A mouse had a positive impact on survival, disease onset, disease progression and on a number of cellular and biochemical readouts of ALS. We generated here SOD1G93A mice with reduced expression of mGluR5 (SOD1G93AGrm5-/+) by crossing the SOD1G93A mutant mouse with the mGluR5 heterozigous Grm5-/+ mouse. SOD1G93AGrm5-/+ mice showed prolonged survival probability and delayed pathology onset. These effects were associated to enhanced number of preserved MNs, decreased astrocyte and microglia activation, reduced cytosolic free Ca2+ concentration, and regularization of abnormal Glu release in the spinal cord of SOD1G93AGrm5-/+ mice. Unexpectedly, only male SOD1G93AGrm5-/+ mice shown improved clinical disease progression vs. SOD1G93A mice, while SOD1G93AGrm5-/+ females did not. These results demonstrate that a lower constitutive level of mGluR5 has a significant positive impact in mice with ALS and support the idea that blocking Group I mgluRs may represent a potentially effectual pharmacological approach to ALS.

*Title page

In-vivo effects of knocking-down metabotropic glutamate receptor 5 in the *SOD1^{G93A}* mouse model of amyotrophic lateral sclerosis

[1#]Tiziana Bonifacino, [1#]Luca Cattaneo, [1]Elena Gallia, [2,3,4]Aldamaria Puliti, [5,6]Marcello Melone, [1]Francesca Provenzano, [2]Simone Bossi, [2,7]Ilaria Musante, [8]Cesare Usai, [5,6]Fiorenzo Conti, [1,4]Giambattista, Bonanno, [1,4]Marco Milanese.

[#] Equally contributed

[1]Department of Pharmacy, Unit of Pharmacology and Toxicology, University of Genoa Viale Cembrano, 4 - 16148, Genoa, Italy. [2]Department of Neuroscience, Rehabilitation, Ophthalmology, Genetics and Maternal and Child Health, L.go P. Daneo, 3 - 16132, Genoa, Italy. [3]Medical Genetics Unit, Istituto Giannina Gaslini, Via G. Gaslini, 5 - 16147, Genoa, Italy. [4]Centre of Excellence for Biomedical Research, University of Genoa, Viale Benedetto XV, 9 - 16132, Genoa, Italy. [5]Department of Experimental and Clinical Medicine, Unit of Neuroscience and Cell Biology, Università Politecnica delle Marche, Via Tronto 10/a – 60126, Torrette di Ancona, Ancona, Italy. [6]Centre for Neurobiology of Aging, INRCA IRCCS, Via S.Margherita, 5 - 60124, Ancona, Italy. [7]Telethon Institute for Genetics and Medicine, Via Campi Flegrei, 32 – 80078, Pozzuoli, Napoli, Italy (present Institution for IM). [8]Institute of Biophysics, National Research Council (CNR), Via De Marini, 6 - Torre di Francia - 16149, Genoa, Italy.

Corresponding author:

Prof. Giambattista Bonanno, University of Genoa, Department of Pharmacy, Viale Cembrano 4, 16148 Genoa, Italy. Tel: +39 010 3532658. bonanno@difar.unige.it

ABSTRACT

Amyotrophic lateral sclerosis (ALS) is a fatal neurodegenerative disorder due to loss of upper and lower motor neurons (MNs). The mechanisms of neuronal death are largely unknown, thus prejudicing the successful pharmacological treatment. One major cause for MN degeneration in ALS is represented by glutamate(Glu)-mediated excitotoxicity. Activation of Group I metabotropic Glu receptors (mGluR1 and mGluR5) at glutamatergic spinal cord nerve terminals has been reported to produce abnormal Glu release in the widely studied *SOD1*^{G93A} mouse model of ALS. We also reported that halving mGluR1 expression in the *SOD1*^{G93A} mouse had a positive impact on survival, disease onset, disease progression and on a number of cellular and biochemical readouts of ALS. We generated here *SOD1*^{G93A} mice with reduced expression of mGluR5 (*SOD1*^{G93A}*Grm5*$^{-/+}$) by crossing the *SOD1*^{G93A} mutant mouse with the mGluR5 heterozigous *Grm5*$^{-/+}$ mouse. *SOD1*^{G93A}*Grm5*$^{-/+}$ mice showed prolonged survival probability and delayed pathology onset. These effects were associated to enhanced number of preserved MNs, decreased astrocyte and microglia activation, reduced cytosolic free Ca^{2+} concentration, and regularization of abnormal Glu release in the spinal cord of *SOD1*^{G93A}*Grm5*$^{-/+}$ mice. Unexpectedly, only male *SOD1*^{G93A}*Grm5*$^{-/+}$ mice shown improved clinical disease progression vs. *SOD1*^{G93A} mice, while *SOD1*^{G93A}*Grm5*$^{-/+}$ females did not. These results demonstrate that a lower constitutive level of mGluR5 has a significant positive impact in mice with ALS and support the idea that blocking Group I mgluRs may represent a potentially effectual pharmacological approach to ALS.

In-vivo effects of knocking-down metabotropic glutamate receptor 5 in the *SOD1^{G93A}* mouse model of amyotrophic lateral sclerosis

[1#]Tiziana Bonifacino, [1#]Luca Cattaneo, [1]Elena Gallia, [2,3,4]Aldamaria Puliti, [5,6]Marcello Melone, [1]Francesca Provenzano, [2]Simone Bossi, [2,7]Ilaria Musante, [8]Cesare Usai, [5,6]Fiorenzo Conti, [1,4*]Giambattista, Bonanno, [1,4]Marco Milanese.

[#] Equally contributed

[1]Department of Pharmacy, Unit of Pharmacology and Toxicology, University of Genoa Viale Cembrano, 4 - 16148, Genoa, Italy. [2]Department of Neuroscience, Rehabilitation, Ophthalmology, Genetics and Maternal and Child Health, L.go P. Daneo, 3 - 16132, Genoa, Italy. [3]Medical Genetics Unit, Istituto Giannina Gaslini, Via G. Gaslini, 5 - 16147, Genoa, Italy. [4]Centre of Excellence for Biomedical Research, University of Genoa, Viale Benedetto XV, 9 - 16132, Genoa, Italy. [5]Department of Experimental and Clinical Medicine, Unit of Neuroscience and Cell Biology, Università Politecnica delle Marche, Via Tronto 10/a – 60126, Torrette di Ancona, Ancona, Italy. [6]Centre for Neurobiology of Aging, INRCA IRCCS, Via S.Margherita, 5 - 60124, Ancona, Italy. [7]Telethon Institute for Genetics and Medicine, Via Campi Flegrei, 32 – 80078, Pozzuoli, Napoli, Italy (present Institution for IM). [8]Institute of Biophysics, National Research Council (CNR), Via De Marini, 6 - Torre di Francia - 16149, Genoa, Italy.

*Corresponding author:
Prof. Giambattista Bonanno, University of Genoa, Department of Pharmacy, Viale Cembrano 4, 16148 Genoa, Italy. Tel: +39 010 3532658. bonanno@difar.unige.it

ABSTRACT

Amyotrophic lateral sclerosis (ALS) is a fatal neurodegenerative disorder due to loss of upper and lower motor neurons (MNs). The mechanisms of neuronal death are largely unknown, thus prejudicing the successful pharmacological treatment. One major cause for MN degeneration in ALS is represented by glutamate(Glu)-mediated excitotoxicity. Activation of Group I metabotropic Glu receptors (mGluR1 and mGluR5) at glutamatergic spinal cord nerve terminals has been reported to produce abnormal Glu release in the widely studied *SOD1*^{G93A} mouse model of ALS. We also reported that halving mGluR1 expression in the *SOD1*^{G93A} mouse had a positive impact on survival, disease onset, disease progression and on a number of cellular and biochemical readouts of ALS. We generated here *SOD1*^{G93A} mice with reduced expression of mGluR5 (*SOD1*^{G93A}*Grm5*$^{-/+}$) by crossing the *SOD1*^{G93A} mutant mouse with the mGluR5 heterozigous *Grm5*$^{-/+}$ mouse. *SOD1*^{G93A}*Grm5*$^{-/+}$ mice showed prolonged survival probability and delayed pathology onset. These effects were associated to enhanced number of preserved MNs, decreased astrocyte and microglia activation, reduced cytosolic free Ca^{2+} concentration, and regularization of abnormal Glu release in the spinal cord of *SOD1*^{G93A}*Grm5*$^{-/+}$ mice. Unexpectedly, only male *SOD1*^{G93A}*Grm5*$^{-/+}$ mice shown improved clinical disease progression vs. *SOD1*^{G93A} mice, while *SOD1*^{G93A}*Grm5*$^{-/+}$ females did not. These results demonstrate that a lower constitutive level of mGluR5 has a significant positive impact in mice with ALS and support the idea that blocking Group I mgluRs may represent a potentially effectual pharmacological approach to ALS.

KEYWORDS

Amyotrophic lateral sclerosis
SOD1^{G93A} mouse model
Metabotropic glutamate receptor type 5
Metabotropic glutamate receptor type 5 knock down
Glutamate transmission
Clinical disease progression

ABBREVIATIONS

AMPA, α-amino-3-hydroxy-5-methyl-4-isoxazole propionate
[^{3}H]D-Asp, [^{3}H]D-aspartate
3,5-DHPG, (S)-3,5-dihydroxyphenylglycine
Gapdh, Glyceraldehyde 3-phosphate dehydrogenase
mGluR1, metabotropic glutamate receptor 1
mGluR5, metabotropic glutamate receptor 5
MN, motoneuron
NMDA, N-methyl-D-aspartate

INTRODUCTION

Amyotrophic lateral sclerosis (ALS) is a lethal neurodegenerative disease characterized by rapid and progressive motor neuron (MN) death and glial cell degeneration in the spinal cord, brainstem, and motor cortex, which result into weakness, muscle atrophy and spasticity (Eisen, 2009).

ALS is mostly sporadic, although familial forms have been reported in about 5-10% of cases (Byrne et al., 2011). At present, at least fifteen genes coding for different proteins and involved in the regulation of numerous cellular pathways have been associated to ALS (Andersen and Al-Chalabi, 2011). A large percentage of patients with familial ALS present mutations of superoxide dismutase-1 (SOD1), the first identified ALS-linked protein (Rosen et al., 1993), which is implicated in about 25% of familiar ALS cases. Over 170 different mutations in the SOD1 protein have been identified, most of them causally linked to familiar ALS (Pasinelli and Brown, 2006; Kaur et al., 2016). Thus, even though that pathogenic mechanisms are still elusive, multiple cellular events may contribute to the disease. Certainly, ALS is a complex multifactorial disease, involving several intracellular pathological processes (Ferraiuolo et al., 2011; Peters et al., 2015) and neuronal and non-neuronal cell types (Ilieva et al., 2009).

In this scenario, altered excitatory neurotransmission plays a key role in the disease progression (Van Den Bosch et al., 2006), as sustained by preclinical evidence in *SOD1*^{G93A} mice (Alexander et al., 2000) and clinical studies in ALS patients (Shaw et al., 1995; Wuolikainen et al., 2011) showing that the extracellular concentration of glutamate (Glu) is increased in the spinal cord, plasma and cerebrospinal fluid. Different causes may sustain the increased Glu levels, including reduced efficiency of Glu transport (Rothstein et al., 1995, 2005) and increased Glu release (Milanese et al., 2011; Giribaldi at al., 2013; Bonifacino et al., 2016).

The molecular targets of Glu are ionotropic receptors, comprising NMDA, AMPA and kainate receptors (Dingledine et al., 1999), and metabotropic receptors (mGluRs), which form a family of eight subtypes, divided into three groups. Group II, which includes mGluR2 and mGluR3, and group III, which includes mGluR4, mGluR6, mGluR7, and mGluR8 are inhibitory and negatively coupled to adenylyl cyclase activity; Group I receptors, which includes mGluR1 and mGluR5, are excitatory and their activation produces inositol-1,4,5-trisphosphate and diacylglycerol, with ensuing mobilization of intracellular Ca^{2+} and activation of protein kinase C (Pin and Duvoisin, 1995; Nicoletti et al., 2011). Group I metabotropic Glu receptors are actively involved in the regulation of important cellular pathways and several reports described mGluR1 and mGluR5 over-expression in the spinal cord of ALS patients and *SOD1*^{G93A} mice (Aronica et al., 2001; Valerio et al., 2002), where they are implicated as contributing to degeneration of glial and neuronal cells (Valerio et al., 2002; Rossi et al., 2008; D'Antoni et al., 2011).

We have recently reported that activation of presynaptic mGluR1 and mGluR5 autoreceptors by submicromolar concentrations of the mixed mGluR1/5 agonist 3,5-Dihydroxyphenylglycine (3,5-DHPG), promoted excessive Glu release in the spinal cord of *SOD1*^{G93A} mice (Giribaldi et al, 2013). Building on this background, we also investigated whether this excessive mGluR1 activity plays a role in the pathogenesis of ALS. To this end, we have obtained double mutant mice expressing the *SOD1*^{G93A} human protein and partially lacking mGluR1 (*SOD1*^{G93A}*cerv4*$^{-/+}$). Interestingly, halving the expression of mGluR1 in *SOD1*^{G93A} mouse genetic background increased survival and ameliorated disease hallmarks, including clinical symptom progression (Milanese et al., 2014).

Here we explored the in-vivo effect of reducing the expression of mGluR5 in the *SOD1*^{G93A} mice. We found that double mutant mice, expressing the *SOD1*^{G93A} mutated gene and heterozigous for the mGluR5 inactivating mutation (*SOD1*^{G93A}*Grm5*$^{-/+}$) proved delayed disease onset, increased survival probability, protected MNs from death, and improved

biochemical and histological readouts of the disease state. Unexpectedly, only male *SOD1*^{G93A}*Grm5*$^{-/+}$mice showed amelioration also of clinical symptoms.

MATERIALS AND METHODS

Animals

B6SJL-Tg(SOD1*G93A)1Gur mice expressing high copy number of mutant human SOD1 with a Gly93Ala substitution (*SOD1*^{G93A} mice; Gurney et al., 1994) and B6;129-Grm5^{tm1Rod}/J, carrying a null mutation for mGluR5 (*Grm5*$^{-/+}$; Lu et al., 1997) were originally obtained from Jackson Laboratories (Bar Harbor, ME, USA). *SOD1*^{G93A} mouse colony was maintained by crossing *SOD1*^{G93A} male mice with background-matched B6SJL wild-type (WT) females and selective breeding preserved the transgene in the hemizygous state. Mice carrying the *SOD1*^{G93A} mutation were identified analyzing tissue extracts from tail tips as previously described (Raiteri et al., 2004). Tissue was homogenized in phosphate-buffer saline, freeze/thawed twice and centrifuged at 23,000 x *g* for 15 min at 4° C and the SOD1 level was evaluated by staining for its enzymatic activity after 10% non denaturing polyacrylamide gel electrophoresis. The genotype of *Grm5*$^{-/+}$ mice was identified by polymerase chain reaction (PCR) using specific primers according to the Jackson Laboratory protocols with minor modifications. Briefly, DNA was extracted from mice tails according to the manufacturer's protocol (KAPA Mouse Genotyping Kits, Kapa Biosystems, Woburn, MA, USA) and amplified using 2 couples of primers. The first one (5'-CACATGCCAGGTGACATTAT-3' and 5'-CCATGCTGGTTGCAGAGTAA-3') that amplifies a product of 442 bp for the WT alleles. The second couple of primers (5'-CCCTAGAGCAAAGCATTGAGTT-3' and 5'-GCCAGAGGCCACTTGTGTAG-3') amplifies a genomic fragment of 254 bp specific for the gene target insertion of the *Grm5* null gene.

SOD1^{G93A} male mice (on a mixed C57BL6-SJL background) were bred with *Grm5*$^{-/+}$ females to generate *SOD1*^{G93A}*Grm5*$^{-/+}$ double-mutants carrying the *Grm5*$^{-/+}$ heterozygous mutation and the SOD*1*G93A* transgene. All experiments were conducted on littermates derived from this last breeding (Fig. 1). Animals were housed at constant temperature (22 ± 1°C) and relative humidity (50%) with a regular 12 h-12 h light cycle (light 7 AM-7 PM), throughout the experiments. Food (type 4RF21 standard diet obtained from Mucedola, Settimo Milanese, Milan, Italy) and water were freely available.

Experiments were carried out in accordance with the guidelines established by the European Communities Council (EU Directive 114 2010/63/EU for animal experiments published on September 22nd, 2010) and with the Italian D.L. n. 26/2014, and were approved by the local Ethical Committee and the Italian Ministry of Health (Prot. No. 31754-3). All efforts were made to minimize animal suffering and to use only the number of animals necessary to produce reliable results. Sexes were balanced in each experimental group to avoid bias due to sex-related intrinsic differences in disease severity. For experimental use animals were killed at a late stage of disease, scored according to motor impairment severity (Uccelli et al., 2012). A total number of 41 WT, 88 *SOD1*^{G93A}, 100 *SOD1*^{G93A}*Grm5*$^{-/+}$, and 21 *Grm5*$^{-/+}$ mice were utilized in this study. Both male and female animals were used and sexes were balanced in each experimental group.

Survival and motor performance

Survival time was identified as the time at which mice were unable to right itself within 20 s when placed on their side. Survival data originated from animals that did not underwent behavioural studies in order to avoid their influence on disease progression. In principle, animals used in behavioural tests were not used for other experiments. The effects of the genetic manipulation on clinical onset and disease symptoms were analysed by Rotarod and motor deficit tasks. Clinical test registration was started at day 90 and data were

recorded three times a week, until the end of the experiments, in WT, *SOD1*^{G93A}, *Grm5*$^{-/+}$, and *SOD1*^{G93A}*Grm5*$^{-/+}$ mice. Tests were performed in randomized order by a blinded observer. Rotarod test: the time for which an animal could remain on the rotating cylinder was measured using an accelerating Rotarod apparatus (RotaRod 7650; Ugo Basile, Comerio, Italy). In this procedure the rod rotation gradually increases in speed from 4 to 40 r.p.m. over the course of 5 min. The time that the mice stayed on the rod until falling off was recorded. Before registration animals were trained for 10 days. Motor deficits: mice were rated for disease progression by scoring the extension reflex of hind limbs and the gait impairment. In the extension reflex test, animals were evaluated by observing the hind limbs posture when suspended by the tail. Gait deficits were measured by observing mice in an open field. Motor deficits were rated using a 5 point score scale (5, no sign of motor dysfunction; 0, complete impairment) as previously described (Uccelli et al., 2012). Body weight: body weight was measured immediately before behavioural tests. Disease onset was defined retrospectively as the time when mice reached the body weight peak (Boillèe et al., 2006)

Histological studies

WT, *SOD1*^{G93A}, *Grm5*$^{-/+}$ and *SOD1*^{G93A}*Grm5*$^{-/+}$ mice (110-120 days old) were euthanized and spinal cords were post-fixed for 24 h in 4% PFA at 4°C. Then, they were transferred to a solution containing 30% glycerol, 30% ethylene glycol, 30% distilled water and 10% PB and subsequently stored at -20°C. Spinal cords were cut coronally into 50-µm-thick sections with a Vibratome. Sections were collected into groups of ten and one section/group was stained with 0.1% thionine. The lumbar area of spinal cord was identified and the number of 0.1% thionine positive alpha-motor neurons in ventrolateral horn of L4/L5 was estimated by light microscopy, using a Leitz Orthoplan (Wetzlar, Gemany) microscope, in serial 50 µm sections from WT 30 sections/4 animals), *SOD1*^{G93A} mutant (18

sections/3 animals), *Grm5*$^{-/+}$ (8 sections/3 animals) and *SOD1*^{G93A}*Grm5*$^{-/+}$ mice (21 sections/3 animals). Microscopic fields of ventrolateral horns were captured with a digital camera coupled to Leitz Orthoplan microscope; alpha-motoneurons were selected and counted based on diameters greater than 25 μm using ImageJ version 1.29 software (NIH, Bethesda, MD, USA).

Protein expression

Spinal cord from 110-120 days old WT, *SOD1*^{G93A}, *Grm5*$^{-/+}$ and *SOD1*^{G93A}*Grm5*$^{-/+}$ mice were dissected and homogenized in lysis buffer (10 mM Tris, pH 8.8, 20% glycerol, 2% sodium dodecyl sulphate, 0.1 mM EDTA, 5% β-mercaptoethanol). Protein concentration was determined according to Bradford (1976). Appropriate amount (15-20 μg) of total proteins were separated by means of SDS-polyacrylamide gel electrophoresis on 10% precast gel (Bio-Rad, Segrate MI, Italy). The concentration of proteins in each sample felt in the linear portion of the curve. A triplicate analysis for each sample was performed. Electro-blotted proteins were monitored using Naphthol blue black staining (Sigma-Aldrich, St Louis, MO, USA). Membranes were then incubated with the following antibodies: anti-Glial Fibrillar Acidic Protein (GFAP) mouse monoclonal antibody (1:5000; Sigma Aldrich, St Louis, MO, USA); rabbit monoclonal anti-CD11β (1:500; Abcam, Cambridge, UK); anti-mGluR1 mouse monoclonal antibody (1:2500; BD Biosciences, San Jose, CA, USA); anti-mGluR5 rabbit polyclonal (1:10000, Epitomics, Burlingame, CA, USA); mouse monoclonal Anti-Gapdh antibody (1:10000; Millipore, Billerica, MA, USA).

After incubation with appropriate peroxidase-coupled secondary antibodies, protein bands were detected by using a Western blotting detection system (ECL Advance™; Amersham Biosciences, Piscataway, NJ, USA). Bands were detected and analyzed for density using an enhanced chemiluminescence system (Alliance 6.7 WL 20M, UVITEC, Cambridge, UK), and UV1D software (UVITEC). Bands of interest were normalized for

Gapdh level in the same membrane.

Synaptosome purification

Animals (110-120 days old) were euthanized and the whole spinal cord rapidly removed. Synaptosomes were prepared from WT, *SOD1*^{G93A}, *Grm5*$^{-/+}$ and *SOD1*^{G93A}*Grm5*$^{-/+}$ mice essentially as described previously (Milanese et al., 2011). The tissue was homogenized in 14 volumes of 0.32 M sucrose, buffered at pH 7.4 with Tris-HCl, using a glass-teflon tissue grinder (clearance 0.25 mm). The homogenate was centrifuged (5 min, 1,000 x *g* at 4° C) to remove nuclei and debris and the supernatant was gently stratified on a discontinuous Percoll® (Sigma-Aldrich, St Louis, Missouri, USA) gradient (2, 6, 10 and 20% v/v in Tris-buffered sucrose). After centrifugation at 33,500 x *g* for 5 min, the layer between 10 and 20% Percoll® (synaptosomal fraction) was collected, washed (20,000 x *g* for 15 min in physiological medium) and resuspended in physiological medium having the following compositions (mM): NaCl, 140; KCl, 3; $MgSO_4$, 1.2; NaH_2PO_4, 1.2; $NaHCO_3$, 5; $CaCl_2$, 1.2; 4-(2-hydroxyethyl)-1-piperazineethanesulfonic acid (HEPES), 10; glucose, 10; pH 7.4 for $[Ca^{2+}]_c$ determination and release experiments or in lysis buffer for western blotting. Protein was measured according to Bradford (1976) using bovine serum albumin (Sigma-Aldrich, St Louis, Missouri, USA) as a standard. All the reagents were of laboratory grade.

Cytosolic Ca^{2+}

Cyitosolic Ca^{2+} concentration $[Ca^{2+}]_C$ was determined in spinal cord synaptosomes of WT, *SOD1*^{G93A}, *Grm5*$^{-/+}$, and *SOD1*^{G93A}*Grm5*$^{-/+}$ 110-120 days old mice using the fluorescent dye fura-2/AM (Grynkiewicz et al., 1985). Synaptosomes were incubated for 40 min at 37°

C, while gently shaking, in the HEPES-containing physiological medium, in the presence of 20 μM of $CaCl_2$, and 5 μM fura-2/AM dissolved in 0.5% dimethyl sulfoxide (DMSO; Sigma-Aldrich, St Louis, Missouri, USA). Synaptosomes, incubated in the presence of 0.5% dimethyl sulfoxide only, were used to measure auto-fluorescence. After extra-synaptosomal fura-2/AM removal, the pellets were re-suspended in ice-cold standard or Ca^{2+}-free HEPES-buffered medium, divided into 200 μl aliquots (200 μg protein/sample), and stored on ice until use. Measures were obtained within 2 hours.

Synaptosomes were diluted in HEPES-buffered medium containing the appropriate Ca^{2+} concentration (final volume 2 ml) and equilibrated at 37° C for 15 min. The measurements were made at 37° C under continuous stirring using an RF-5301PC dual wavelength spectrofluorophotometer (Shimadzu Corporation, Milan, Italy) by alternating the excitation wavelengths of 340 and 380 nm. Fluorescent emission was monitored at 510 nm. Basal fluorescence was recorded for 1 min, then synaptosomes were exposed to (S)-3,5-Dihydroxyphenylglycine (3,5-DHPG; 0.3 or 30 μM) or to KCl (25 mM) for additional 2 min. Calibration of the fluorescent signals was performed at the end of each measure by adding 10 μM ionomycin in the presence of $CaCl_2$ to obtain F_{max}, followed by 10 mM ethylene glycol tetra acetic acid; adjusted to pH 8.0 with 3 mM; Tris) to obtain F_{min}. After correcting for extracellular dye, $[Ca^{2+}]_c$ was calculated by the equation of Grynkiewicz et al. (1985), using a K_D of 224 nM for the Ca^{2+}-fura-2 complex. All the reagents were of laboratory grade.

Release experiments

Synaptosomes purified from WT, *SOD1*^{G93A}, *Grm5*$^{-/+}$, and *SOD1*^{G93A}*Grm5*$^{-/+}$ 110-120 days old mice were re-suspended in physiological medium and incubated (15 min, 37°C) with 0.05 μM [^{3}H]D-Asp, a non metabolizable analogue of Glu which labels the intra-

terminal releasable pools of the excitatory amino acid (Fleck et al., 2001).

Aliquots were distributed on microporous filters placed at the bottom of a set of 24 parallel superfusion chambers maintained at 37°C (Superfusion System, Ugo Basile, Comerio, Varese, Italy) and processed as previously described (Raiteri et al., 2007). Superfusion was started with physiological medium at a rate of 0.5 ml/min and continued for 48 min. After 36 min of superfusion to equilibrate the system, five 3-min samples were collected and 3,5-DHPG (0.3 or 30 μM) was introduced at the end of the first sample collected (t = 39 min) and maintained until the end of the experiment. In the exeriments of KCl-depolarization, samples were collected according to the following scheme: two 3-min samples (t =36-39 and 45-48 min; basal release) before and after one 6-min sample (t = 39-45 min; stimulus-evoked release). Stimulation with a 90 s pulse of 15 mM KCl was applied at t = 39 min.

Collected samples and superfused synaptosomes were counted for radioactivity. Tritium released in each sample was calculated as fractional rate x 100 (percentage of the total synaptosomal neurotransmitter content at the beginning of the respective collection period). In the experiments of 3,5-DHPG-evoked [^{3}H]D-Asp release, drug effects were evaluated by calculating the ratio between the efflux in the fourth sample collected (in which the maximum effect of 3,5-DHPG was generally reached) and the efflux of the first fraction (basal efflux). This ratio was compared to the corresponding ratio obtained under resting conditions. Release ratios calculated for synaptosomes from WT, *SOD1*^{G93A}, *Grm5*$^{-/+}$, and *SOD1*^{G93A}*Grm5*$^{-/+}$ mice were compared to evaluate the effects of mGluR5 ablation on the 3,5-DHPG evoked [^{3}H]D-Asp release. In the experiments of KCl-evoked [^{3}H]D-Asp release, the stimulus-evoked neurotransmitter overflow was estimated by subtracting the transmitter content in the two 3-min fractions representing the basal release from that in the 6-min fraction collected during and after the stimulating pulse. The overflow values calculated for synaptosomes from the four mouse strains were compared to evaluate the effects of mGluR5

ablation on the depolarization-evoked Glu release. Appropriate controls were always run in parallel.

Statistics

Data are expressed as mean ± s.e.m. and p value < 0.05 was considered significant. The Kaplan–Meier plot was used to evaluate survival probability and cumulative curves were compared using the log-rank test. Statistical comparison of two means were performed by unpaired two-tailed Student's t-test while multiple comparisons were performed using the analysis of variance (ANOVA) followed by Bonferroni post hoc test. Analyses were performed by means of SigmaStat (Systat Software, Inc., San Jose, CA, USA) software.

RESULTS

Generation of *SOD1^{G93A}Grm5$^{-/+}$* mice

To obtain mice expressing high copy number of human G93A-mutated SOD1 and half dose of mGluR5, we crossed *SOD1^{G93A}* transgenic mice with the *Grm5$^{-/+}$* mouse line (see Fig. 1). WT, Grm5$^{-/+}$, *SOD1^{G93A}*, and *SOD1^{G93A}Grm5$^{-/+}$* were all born at the expected Mendelian ratio and were indistinguishable from wild-type littermates at birth. Spinal cord lysates of *SOD1^{G93A}Grm5$^{-/+}$* and *SOD1^{G93A}* mice were analysed for mGluR1 and mGluR5 expression, showing that mGluR5 was half in *SOD1^{G93A}Grm5$^{-/+}$* than in *SOD1^{G93A}* mice (about 45% of reduction; p=0.007, $t_{(10)}$=3.419) while mGluR1 was unmodified (Fig. 2A). A similar result was detected in *Grm5$^{-/+}$* compared to WT mice: mGluR5 was reduced in *Grm5$^{-/+}$* (about 60%; p=0.003, $t_{(10)}$=3.996) and mGluR1 remained unchanged (Fig. 2B).

Survival probability and weight loss in *SOD1^{G93A}Grm5$^{-/+}$* mice

Survival probability and weigh loss have been calculated by using 39 *SOD1^{G93A}* mice (21 male and 18 female) compared with 46*SOD1^{G93A}Grm5$^{-/+}$* mice (25 male and 21 female). Animal used in this set of experiments were not subjected to any other assay. Halving mGluR5 expression significantly prolonged life span of *SOD1^{G93A}Grm5$^{-/+}$* double mutants compared to SOD1^{G93A} mice. The survival age mean of *SOD1^{G93A}* mice was 134 ± 1.50 days and it was shifted to 153 ± 1.54 days in the case of *SOD1^{G93A}Grm5$^{-/+}$* mice ($p<0.001$, $t_{(83)}$=-8.932). The Kaplan-Meier graph reported in Fig. 3A shows a significant ($p<0.001$) survival probability amelioration in of *SOD1^{G93A}Grm5$^{-/+}$* respect to *SOD1^{G93A}* mice. The analysis of the sex contribution to the above results revealed that the survival age mean of male *SOD1^{G93A}* mice was 131 ± 2.15 days and it was shifted to 154 ± 2.20 days in the case of *SOD1^{G93A}Grm5$^{-/+}$* mice ($p<0.001$, $t_{(44)}$=-7.513) (Fig. 3B). Female *SOD1^{G93A}Grm5$^{+/-}$* mice exhibited a less pronounced shift of the survival curve (Fig.3C) when compared to male *SOD1^{G93A}Grm5$^{-/+}$* mice. The survival age mean of female *SOD1^{G93A}* mice was 138 ± 1.83 days and it was shifted to 153 ± 2.56 days in the case of *SOD1^{G93A}Grm5$^{-/+}$* mice ($p<0.001$, $t_{(36)}$=-4.633). The survival probability amelioration shown in Figures. 3B and 3C, estimated by the Kaplan-Meier method was always statistically significant ($p<0.001$)

Male and female *SOD1^{G93A}* mice showed a significant decrease of body weight starting at day 114 ($p<0.05$, $t_{(23)}$=-2.228) or at day 120 ($p<0.05$, $t_{(23)}$=-2.358), respectively, when compared to WT mice (Figs. 4A and B). The body weight decrease was delayed in *SOD1^{G93A}Grm5$^{-/+}$* mice, turning out to be significant at day 132 both in male and female mice ($p<0.05$, $t_{(26)}$=-2.138) ($p<0.05$, $t_{(26)}$=-2.138 and $p<0.05$, $t_{(23)}$=-2.226 respectively). Weight decrease was always less pronounced in *SOD1^{G93A}Grm5$^{-/+}$* than in *SOD1^{G93A}* mice during lifespan.

The delayed weight loss, which has been linked to the onset of symptoms (Boillée et

al., 2006), and the delayed death inception in *SOD1^{G93A}Grm5$^{-/+}$* mice suggest that halving the expression of mGluR5 in *SOD1^{G93A}* mice postpones the clinical progress of the disease.

Motor functions in *SOD1^{G93A}Grm5$^{-/+}$* mice

To monitor disease progression, the motor performances of *SOD1^{G93A}* and *SOD1^{G93A}Grm5$^{-/+}$* mice were assessed by Rotarod, extension reflex and gait impairment tasks (Milanese et al., 2014) by using 28 *SOD1^{G93A}* mice (13 male and 15 female) and 33 *SOD1^{G93A}Grm5$^{-/+}$* mice (15 male and 18 female). In details, the performance of *SOD1^{G93A}* and *SOD1^{G93A}Grm5$^{-/+}$* mice in the three tasks scrutinized were superimposable to that of *WT* mice until around day 80 (not shown in the figure), then they rapidly worsened, as expected. In this latter phase, *SOD1^{G93A}Grm5$^{-/+}$* mice apparently did not perform significantly better than *SOD1^{G93A}* mice, although a tendency to amelioration could be observed in Rotarod (Fig. 5A), extension reflex (Fig. 6A), and gait (Fig. 7A). Interestingly, a significant amelioration of the three tasks was observed in male *SOD1^{G93A}Grm5$^{-/+}$* mice (Fig. 5B, 6B, 7B). No differences were observed in female *SOD1^{G93A}Grm5$^{-/+}$* mice (Fig. 5C, 6C, 7C) compared to *SOD1^{G93A}* animals.

Thus, halving the expression of mGluR5 in *SOD1^{G93A}* mice slowed down the neurological phenotype progression only in *SOD1^{G93A}Grm5$^{-/+}$* male mice.

Motor neuron preservation in *SOD1^{G93A}Grm-5$^{-/+}$* mice

The progressive loss of spinal MNs is one of the main features of ALS. We determined here the number of MNs using WT, *SOD1^{G93A}*, *Grm5$^{-/+}$* and *SOD1^{G93A}Grm5$^{-/+}$* mice (aged 110-120 days) in thionine-stained sections from the ventral horns of lumbar spinal cord at the L4/L5 level. Figure 8A shows that WT and *Grm5$^{-/+}$* mice displayed comparable gross histological characteristics. In contrast, *SOD1^{G93A}* mice showed low tissue preservation and severe MN loss**,** while *SOD1^{G93A}Grm5$^{-/+}$* mice exhibited intermediate

histology and MN number. As shown in Figure 8B, the number of MNs in the ventrolateral horn of spinal cord was 24.9 ± 0.7 in WT, 8 ± 0.4 in *SOD1*^{G93A}, 24.4 ± 0.7 in *Grm5*$^{-/+}$, and 14.6 ± 0.5 in *SOD1*^{G93A}*Grm5*$^{-/+}$ mice.

Thus, the number of MNs was significantly preserved in *SOD1*^{G93A}*Grm5*$^{-/+}$ late symptomatic mice, compared to age matched *SOD1*^{G93A} mice ($p<0.001$, $F_{(8,11)}=191.969$). This result is in line with the increased survival probability but apparently mismatches with the above motor ability results.

Astroglia and microglia activation state in *SOD1*^{G93A}*Grm-5*$^{-/+}$ mice

Astrogliosis and microgliosis have been described in ALS (Rossi et al., 2008; Lasiene and Yamanaka, 2011). We detected reactive astroglia and microglia in the spinal cord of 110-120 days old WT, *SOD1*^{G93A}, *Grm5*$^{-/+}$ and *SOD1*^{G93A}*Grm5*$^{-/+}$ mice by measuring the expression of the markers GFAP and CD-11β, respectively. GFAP expression was almost doubled in *SOD1*^{G93A} mice, respect to WT and *Grm5*$^{-/+}$ mice, which did not greatly differ each other. Interestingly, GFAP over-expression was significantly reduced in *SOD1*^{G93A}*Grm5*$^{-/+}$mice respect to *SOD1*^{G93A} mice ($p<0.001$, $F_{(3,22)}=20.217$) (Fig. 9A). The expression of CD-11β was barely detectable in WT and *Grm5*$^{-/+}$, indicating very low microglia activation under control conditions, but it was greatly enhanced in *SOD1*^{G93A} mice. Similarly to astrogliosis, also the expression of CD-11β was significantly reduced in *SOD1*^{G93A}*Grm5*$^{-/+}$ mice ($p<0.001$, $F_{(8,11)}=69.660$) (Fig. 9B).

These results suggest that halving the expression of mGluR5 ameliorates the astrocytosis and microgliosis present in *SOD*^{G93A} mice, producing a more favourable environment for MNs.

Calcium homeostasis in *SOD1*^{G93A}*Grm5*$^{-/+}$ mice.

We have previously shown that $[Ca^{2+}]_C$ is increased in the cytoplasm of spinal cord

nerve terminals of *SOD1*^{G93A} mice, both at pre-symptomatic and symptomatic stages of disease (Bonifacino et al., 2016; Milanese et al., 2011). Here we investigated whether knocking-down mGluR5 could modify the basal and the stimulus evoked $[Ca^{2+}]_C$ in *SOD1*^{G93A} mice. $[Ca^{2+}]_C$ was measured in spinal cord synaptosomes of 110-120 days old WT, *Grm5*$^{-/+}$, *SOD1*^{G93A} and *SOD1*^{G93A}*Grm5*$^{-/+}$ mice by means of the fluorescent dye Fura2/AM.

The $[Ca^{2+}]_C$ in WT mice amounted to 163.46 ± 8.33 nM under basal conditions and it did not differ significantly from *Grm5*$^{-/+}$ mice (165.59 ± 18.81 nM). Basal $[Ca^{2+}]_C$ was significantly higher, in *SOD1*^{G93A} mice (256.70 ± 2.65 nM; $p<0.001$, $F_{(3,25)}=15.679$). This elevated basal $[Ca^{2+}]_C$ was significantly reduced in *SOD1*^{G93A}*Grm5*$^{-/+}$ mice (211.25 ± 9.45 nM; $p<0.05$, $F_{(3,25)}=15.679$), which it did not differ statistically from controls (Figure 10A).

We then measured the effects of the mixed mGluR1/5 agonist 3,5-DHPG on $[Ca^{2+}]_C$. Exposure to 0.3 μM of the agonist increased $[Ca^{2+}]_C$ to 365.30 ± 4.06 nM in WT mice, a value that was superimposable to that in *Grm5*$^{+/-}$ mice (360 ± 5.03 nM) (see Fig. 10A for basal values). 3,5-DHPG stimulation enhanced $[Ca^{2+}]_C$ in *SOD1*^{G93A} mice even to a greater extent (526.50 ± 7.50 nM; $p<0.001$, $F_{(3,15)}=18.961$ vs. WT mice) and this effect was significantly reduced, in *SOD1*^{G93A}*Grm5*$^{-/+}$ mice (451.20 ± 20.68 nM; $p<0.05$, $F_{(3,15)}=18.961$). Figure 10B shows that also 30 μM DHPG augmented $[Ca^{2+}]_C$ in WT and *Grm5*$^{-/+}$ control mice (405.20 ± 22 nM and 400.70 ± 5.21 nM, respectively) and this effect was significantly higher in *SOD1*^{G93A} mice (607.30 ± 2.19 nM; $p<0.001$, $F_{(3,11)}=344.111$ vs WT mice). Of note, differently from 0,3 μM DHPG, in the presence of the 30 μM DHPG $[Ca^{2+}]_C$ did not change in *SOD1*^{G93A}*Grm5*$^{-/+}$ (582.10 ± 3.04 nM) respect to *SOD1*^{G93A}.

Finally, we investigated the possibility that knocking-down mGluR5 could also modify $[Ca^{2+}]_C$ changes due to stimuli other than Group I mGluR activation. At this purpose, we studied the effects of high KCl depolarization, which induces excessive Glu release in the spinal cord of *SOD1*^{G93A} mice (Milanese et al., 2011; Bonifacino et al., 2016). Figure 10C

shows that 25 mM KCl almost doubled the basal $[Ca^{2+}]_C$ in WT as well as in *Grm5*$^{-/+}$ mice (315.20 ± 33.62 nM and 319 ± 39 nM, respectively) (see Fig. 10A for basal values). Exposure to high KCl provoked a further increase of $[Ca^{2+}]_C$ in *SOD1*^{G93A} (471.70 ± 28 nM; $p<0.05$, $F_{(3,8)}=6.949$) and this effect was abolished in *SOD1*^{G93A}*Grm5*$^{-/+}$ mice (325 ± 15.90 nM; $p<0.05$, $F_{(3,8)}=6.949$).

Thus, halving the expression of mGluR5 in *SOD1*^{G93A} mice diminishes the abnormal $[Ca^{2+}]_C$ either under basal or after DHPG and KCl stimulation in spinal cord synaptosomes, suggesting that this receptor plays a role in shaping intra-terminal Ca^{2+} fluxes and fostering the aptitude of these terminals to produce exocytotic neurotransmitter release.

[^{3}H]D-aspartate release in *SOD1*^{G93A}*Grm5*$^{-/+}$ mice

We have previously demonstrated that exocytotic Glu release is abnormal in the spinal cord of pre-symptomatic and symptomatic *SOD1*^{G93A} mice (Milanese et al., 2011; Bonifacino et al., 2016). We also found that activation of pre-synaptic mGlu1/5 autoreceptors also provokes excessive Glu release, thus triggering Glu-induced-Glu release (Giribaldi et al., 2013).

To explore the possibility that the above reported $[Ca^{2+}]_C$ modifications after mGluR5 knocking down could affect Glu release in *SOD1*^{G93A} mice, we monitored the basal and the DHPG- or high KCl-induced release of [^{3}H]D-Asp, used to label the intra-terminal releasing pools of Glu (Fleck et al., 2001), in synaptosomes isolated from the spinal cord of 110-120 days old WT, *Grm5*$^{-/+}$, *SOD1*^{G93A} and *SOD1*^{G93A}*Grm5*$^{-/+}$ mice.

Either basal release (Fig. 11A), 0.3 and 30 μM 3,5-DHPG-induced (Fig. 11B) or 15 mM KCl-evoked (Fig. 10C) overflow of [^{3}H]D-Asp was significantly elevated in *SOD1*^{G93A} respect to WT mice (basal release, about 76% increase, $p<0.001$, $F_{(3,33)}=15.805$; 0.3 μM 3,5-DHPG, 135% increase, $p<0.05$, $F_{(3,19)}=6.228$; 30 μM 3,5-DHPG, 49% increase, $p<0.05$,

$F_{(3,26)}$=6.323; , 15 mM KCl, 74% increase, $p<0.05$, $F_{(1,3,3,28)}$=1.939), as already described. On the contrary, no differences were observed comparing [^{3}H]D-Asp release in *Grm5*$^{-/+}$ and WT mice under basal conditions or after stimulation with 3,5-DHPG or high KCl (Fig. 11A-C).

Figure 11A also shows that reducing mGluR5 expression in *SOD1*^{G93A}*Grm5*$^{-/+}$ mice significantly reduced the excessive release of [^{3}H]D-Asp measured under resting condition in *SOD1*^{G93A} mice ($p<0.05$, $F_{(3,33)}$=15.805). Similarly, the excessive [^{3}H]D-Asp release induced by 0.3 or 30 μM 3,5-DHPG in *SOD1*^{G93A} mice was abolished in *SOD1*^{G93A}*Grm5*$^{-/+}$ mice, ($p<0.05$, $F_{(3,19)}$=6.228 and $F_{(3,26)}$=6.323, respectively; Fig. 11B). Figure 11C shows that also the abnormal ^{3}[H]D-Asp release induced by high KCl depolarization, present in *SOD1*^{G93A} mice, was abolished in *SOD1*^{G93A}*Grm5*$^{-/+}$ double mutants ($p<0.05$, $F_{(1,3,3,28)}$=1.939).

Thus, halving mGluR5 expression in the *SOD1*^{G93A} background dampens the abnormal Group I mGluR-induced [^{3}H]D-Asp release. Interestingly, knocking down mGlu5 receptors also reduced the KCl-evoked excessive Glu release, bridging in this way the two phenomena.

DISCUSSION

Knocking-down mGluR5 in the *SOD1*^{G93A} mouse model of human ALS delays the disease onset and prolongs survival probability, protects MNs from death and reduces the activation state of astrocytes and microglia, normalizes the augmentation of $[Ca^{2+}]_C$ and the excessive release of Glu, reported to occurs during disease progression. Surprisingly, the genetic interference produces positive effects on motor impairment in male *SOD1*^{G93A}*Grm5*$^{-/+}$ mice only.

In this respect, the results obtained with *SOD1*^{G93A}*Grm5*$^{-/+}$ mice differ from those previously reported in *SOD1*^{G93A}*Grm1*$^{cerv4/+}$ mice, heterozygous for a genetic inactivating mutation of mGluR1 coding gene (crv4) (Conti et al., 2006; Rossi et al., 2013) In details, survival probability significantly improved in mixed male and female *SOD1*^{G93A}*Grm1*$^{cerv4/+}$ vs. *SOD1*^{G93A} mice (Milanese et al., 2014) and no evident sex differences were found (data not shown). The same, Rotarod, extension reflex and gait curves were significantly shifted to the right in mixed male and female *SOD1*^{G93A}*Grm1*$^{cerv4/+}$ mice respect to *SOD1*^{G93A} mice (Milanese et al., 2014), differently from the data here obtained in *SOD1*^{G93A}*Grm5*$^{-/+}$ mice. Despite the smaller number of animals in each behavioural experimental group when separating female and male mice, the motor skill amelioration was still significant in female *SOD1*^{G93A}*Grm1*$^{cerv4/+}$ mice, although less pronounced respect to *SOD1*^{G93A}*Grm1*$^{cerv4/+}$ males (data not shown), at variance of the data described in the present paper.

The reasons of this divergence are not clear. Examining the previous and present results, one difference is that halving mGluR1 expression also led to reduction of mGluR5 (Milanese et al., 2014), while halving mGluR5 expression did not modify mGluR1 (present results). This observation points to mGluR1 playing a central role in motor function preservation in *SOD1*^{G93A} mice. Accordingly, mGluR1 is implicated in the regulation of motor functions in different brain regions, mainly in cerebellum (Swanson and Kalivas,

2000; Nakao et al., 2007), while mGluR5 has not been associated to motor control being instead involved in synaptic plasticity, learning and memory, cognition (Naie and Manahan-Vaughan, 2004; Simonyi et al., 2005). Group I mGluRs are heterogeneously distributed in neuronal and non-neuronal cells in the spinal cord of human and animal models of ALS (Alvarez et al., 2000; Anneser et al., 1999). Autonomic motor neurons from the sacral parasympathetic Onuf's nucleus and thoracic sympathetic neurons, which are spared in ALS, express high levels of mGluR5, while somatic motor neurons do not (Anneser et al., 2004). At variance, vulnerable MNs express high levels of mRNA for mGluR1 while resistant spinal MNs do not (Laslo et al., 2003). In ALS, mGluR5 are over-expressed in ventral spinal cord astrocytes of ALS patients (Aronica et al., 2001), which are more vulnerable to glutamate through a mechanism involving mGluR5 (Rossi et al., 2008). Group I mGluRs are also expressed on microglia where participate in cell migration (Liu et al., 2009) and modulate the inflammatory phenotype (Pinteaux-Jones et al., 2008). Additionally, mGluR5 expression changes during disease progression in *SOD1*^{G93A} mouse spinal cord (Brownell et al., 2015). Finally, it has been reported that male and female mice of different strains may exhibit motor skill differences (Meziane et al., 2007; Kovàcs and Pearce, 2013), which could be possibly magnified by the neurological damage due to the disease. In our tests *SOD1*^{G93A} females performed better than *SOD1*^{G93A} males, and this fact could have minimized the beneficial effect of reducing mGluR5 activity. Therefore, the possible different expression and localization of mGluR1 and mGluR5, the distinct roles of the two receptors, as well as sex-related phenotypes could explain, at least in part, the sex-related dissimilar effect that we obtained by down-regulating mGluR1 or mGluR5 in the *SOD1*^{G93A} mouse model.

The results here presented are in line with the belief that Glu-mediated excitotoxicity is one major pathological determinant in animal models and in individuals with ALS. In this frame, activation of postsynaptic Glu receptors represents a major cause of excitotoxicity.

MNs are particularly sensitive to Glu excitotoxicity triggered by activation of a subset of AMPA receptors that possess unconventional Ca^{2+} permeability because of lack of the edited Q/R GluR2 subunit, whose presence drastically reduces Ca^{2+} entry (Jonas and Burnashew, 1995). Indeed, GluR2 is reduced in murine SOD1 mutants (Laslo et al., 2001; Spalloni et al., 2004) and in spinal cord of ALS individuals (Shaw et al., 1999; Takuma et al., 1999) and this deficit may explain MN vulnerability (Vandenberghe et al., 2000; Van Den Bosh et al., 2000). Studies by our group have pointed to enhanced release as another mechanism for the excessive Glu transmission in ALS. Indeed, we demonstrated that Glu release is abnormally high in the spinal cord of these animals upon exposure to different releasing stimuli, such as activation of heterotransporters (Bonanno and Raiteri 1994) for GABA and Glicine, localized on Glu releasing nerve terminal (Raiteri et al., 2003, 2004, Milanese et al., 2010, 2015), KCl depolarization, ionomicin, hypertonic sucrose (Milanese et al., 2011; Bonifacino et al., 2016) or Group I metabotropic Glu receptors (Giribaldi et al., 2013). Excessive Glu release and modifications or the postsynaptic receptor response in ALS can synergize each other in shaping neurodegeneration.

On the basis of past and recent literature, Glu transmission and excitotoxicity are remarkable topics that is worth to further explore, also considering the new openings represented by the non-cell autonomous nature of the disease (Ilieva et al., 2009), and the newly available animal models of ALS (McGoldrick et al., 2013; Philips and Rothstein, 2016), that may contribute to broad our knowledge and to bring to future focussed human treatments. The limited efficacy of riluzole, that only slightly prolongs survival in ALS patients (Cheung et al., 2006) and whose presumed chief mechanism is to reduce Glu release, may weaken the importance of targeting Glu transmission in the cure. However, although riluzole acts through different mechanisms, it is mainly a Na^{+} channel blocker (Urbani and Belluzzi, 2000; Zona et al., 1998) that non-specifically inhibits the release of

multiple neurotransmitters, either excitatory or inhibitory. A more direct approach to the modulation of Glu transmission should guarantee a greater success.

The reduced expression of mGluR1 (Milanese et al., 2014) as well as of mGluR5 (present results) in *SOD1*^{G93A} mice had favourable consequences on disease progression and survival and on a number of ALS readouts, including Glu release. In other words, mGluR1 and mGluR5 knocking-down can impact on Glu transmission by diminishing both the release of the excitatory amino acid, acting as presynaptic receptors, and the responsiveness of MNs to Glu, acting as postsynaptic receptors and at receptors present on other cells involved in ALS, as astrocytes and microglia. Thus, Group I mGluRs could be included in the Glu receptor repertoire contributing to the over-activation of noxious mechanisms within spinal cord MNs. It would be of interest to define whether also postsynaptic mGluR1 and mGluR5 are over-responsive to Glu, as occurs at presynaptic level. If this were the case, the increased affinity of Group I mGluRs for Glu along with the reported excessive basal release of Glu (Milanese et al., 2011; Bonifacino et al., 2016) may account for tonic activation of pre- and post-synaptic mGluR1 and mGluR5 in *SOD1*^{G93A} mice, that would accompany the phasic over-activation due to the abnormal stimulus-evoked Glu release (Milanese et al., 2011). The presence of an excessive amount of Glu in the synaptic cleft may sustain in turn excessive activation of post-synaptic ionotropic receptors (i.e. AMPA receptors) in a kind of synergic interplay.

Starting from the *in-vitro* finding that the release of Glu induced by mGluR1 and mGluR5 is abnormal in spinal cord synaptosomes of *SOD1*^{G93A} mice (Giribaldi et al., 2013) and from our belief that Group I mGluRs play a role *in-vivo* in experimental ALS, by now verified for mGluR1 (Milanese et al., 2014), we showed here that the abnormal Glu release can be reduced in *SOD1*^{G93A}*Grm5*$^{-/+}$ mice, thus suggesting a causal linkage between Group I mGluR-induced Glu release and the pathology. Indeed, mGluR5 reduction abolished the excessive release of Glu, induced by both 0.3 and 30 μM 3,4-DHPG, indicating that the

partial reduction of mGluR5 is sufficient to abolish the Group 1 mGluR contribution to the over-release. The release of Glu in *SOD1*^{G93A} mice is excessive also after exposure to high KCl, that promotes exocytosis bypassing Glu receptor activation (Milanese et al., 2011). We demonstrated here that down regulating mGluR5 could also significantly decrease the excessive basal release of the excitatory amino acid and abolished that induced by 15 mM KCl, guiding to a unique scenario that brings together the two events.

One effect of glutamate receptor activation is the increase of $[Ca^{2+}]_C$ that is a very precocious hallmark in experimental models of ALS and patients (Siklos et al., 1996; Siklos et al., 1998; Stifanese et al., 2010; Stifanese et al., 2014). Interestingly, mGluR5 knocking-down reduced also the more elevated $[Ca^{2+}]_C$ detected under resting conditions and after stimulation by Group I mGluRs or KCl in *SOD1*^{G93A}, paralleling the effects measured in release experiments. These data suggest that mGluR5 is involved in shaping neuronal $[Ca^{2+}]_C$ and that reducing its expression also reduces the deleterious effects triggered by elevated $[Ca^{2+}]_C$.

Taken together, the above results indicate a possible link between the increase of Glu release and disease progression and suggest that the release of Glu plays a role in the *SOD1*^{G93A} mouse model of ALS; even thought it does not represent the only cause of the pathology since abolishing the excessive Glu release does not entirely prevent from symptoms and death. Other neurotoxic events likely take place at the same time.

ALS is a multifactorial disease, which involves different biochemical pathways associated to multiple cellular events (Peters et al., 2015); hence, each patient may present even unique pathological traits that should be faced by targeting the appropriate biological causes. In spite of the remarkable research in the field, this strategy is at present hindered by the lack of actual biomarkers capable to distinguish patients founding on aetiology and to monitor disease progression (Bowser et al., 2011; Chiò and Traynor, 2014; Simon et al., 2014). Accordingly, a current shared idea is that a successful therapy should be multimodal.

In this scenario, targeting Glu transmission in ALS, for instance operating at mGluR1 and mGluR5, may have the advantage of modifying an up-stream phenomenon, which may in turn affect many down-stream pathways in MNs, mimicking a multimodal therapy.

Conclusions

The present results obtained reducing mGluR5 expression, in the *SOD1*^{G93A} mouse model of ALS, along with previous evidence targeting mGluR1 (Milanese et al., 2014), emphasize the role of Group I mGluRs in the development of ALS and allows proposing the hyper activation of these Glu receptors as a novel mechanism contributing to the disease progression. The reduced expression of mGluR5 determined delayed clinical onset of the disease, amelioration of symptoms, MN preservation, and improved biochemical and functional readouts. Our results suggest that pharmacological treatments aimed at blocking Group I mGluRs can reasonably turn out to be effective in counteracting ALS.

ACKNOWLEDGEMENTS

Foundings: this work was supported by research grants from the Italian Ministry of University (SIR project n.RBSI14B1Z1, to MM).

The authors gratefully acknowledge the undergraduate students: Anna Carle, Giorgio Pastorelli and Rossella Righini, for their very helpful technical support.

CONFLICT OF INTEREST

The authors declare that they have not conflict of interest.

REFERENCE

Alexander, G.,M., Deitch, J.,S., Seeburger, J.,L., Del Valle L., Heiman-Patterson, T.,D., 2000. Elevated cortical extracellular fluid glutamate in transgenic mice expressing human mutant (G93A) Cu/Zn superoxide dismutase. J Neurochem. 74, 1666-1673.

Alvarez, F.,J., Villalba, R.,M., Carr, P.,A., Grandes, P., Somohano, P.,M., 2000. Differential distribution of metabotropic glutamate receptors 1a, 1b, and 5 in the rat spinal cord. J Comp Neurol. 422(3), 464-487.

Andersen, P.,M., and Al-Chalabi, A., 2011. Clinical genetics of amyotrophic lateral sclerosis: what do we really know? Nat. Rev. Neurol., 7, 603-615.

Anneser, J.,M., Borasio, G.,D., Berthele, A., Zieglgänsberger, W., Tölle, T.,R., 1999. Differential expression of group I metabotropic glutamate receptors in rat spinal cord somatic and autonomic motoneurons: possible implications for the pathogenesis of amyotrophic lateral sclerosis. Neurobiol Dis. 6(2),140-147.

Anneser, J.,M., Ince, P.,G., Shaw, P.,J., Borasio, G.,D., 2004. Differential expression of mGluR5 in human lumbosacral motoneurons. Neuroreport. 15(2), 271-273.

Aronica, E., Catania, M.,V., Geurts, J., Yankaya, B., Troost, D., 2001. Immunohistochemical localization of group I and II metabotropic glutamate receptors in control and amyotrophic lateral sclerosis human spinal cord: upregulation in reactive astrocytes. Neuroscience 105, 509–520.

Bonifacino, T., Musazzi, L., Milanese, M., Seguini, M., Marte, A., Gallia, E., Cattaneo, L., Onofri, F., Popoli, M., Bonanno, G., 2016. Altered mechanisms underlying the abnormal glutamate release in amyotrophic lateral sclerosis at a pre-symptomatic stage of the disease. Neurobiol Dis. 95, 122-133.

Bonanno, G. and Raiteri, M., 1994. Release-regulating presynaptic heterocarriers. Progr. Neurobiol. 44, 451-462.

Bowser, R., Turner., M.,R., Shefner, J., 2011. Biomarkers in amyotrophic lateral sclerosis: opportunities and limitations. Nat Rev Neurol 7, 631-638.

Bradford, M.,M., 1976. A rapid and sensitive method for the quantitation of microgram quantities of protein utilizing the principle of protein-dye binding. Anal. Biochem. 72, 248-254.

Brownell, A.,L., Kuruppu, D., Kil, K-E., Jokivarsi, K., Poutiainen, P., Zhu, A., Maxwell, M., 2015. PET imaging studies show enhanced expression of mGluR5 and inflammatory response during progressive degeneration in ALS mouse model expressing SOD1- G93A gene. J Neuroinflammation 12, 217- 225.

Byrne, S., Walsh, C., Lynch, C., Bede, P., Elamin, M., Kenna, K., McLaughlin, R., Hardiman, O.. 2011. Rate of familial amyotrophic lateral sclerosis: a systematic review and meta-analysis. J Neurol. Neurosurg. Psychiatry 82, 623-627.

Cheung, Y.,K., Gordon, P.,H., Levin, B., 2006. Selecting promising ALS therapies in clinical trials. Neurology 67, 1748-1751.

Chiò, A., Traynor, B.,J., 2014. Motor neuron disease in 2014. Biomarkers for ALS-in search of the Promised Land. Nat. Rev. Neurol. 11, 72-74.

Conti, V., Aghaie, A., Cilli, M., Martin, N., Caridi, G., Musante, L., Candiano, G., Castagna, M., Fairen, A., Ravazzolo, R., Guenet, J.,L., Puliti, A., 2006. crv4, a mouse model for human ataxia associated with kyphoscoliosis caused by an mRNA splicing mutation of the metabotropic glutamate receptor 1 (Grm1). Int. J. Mol. Med. 18(4), 593-600.

D'Antoni, S., Berretta, A., Seminara, G., Longone, P., Giuffrida-Stella, A.M., Battaglia, G., Sortino, M.A., Nicoletti, F., Catania, M.V., 2011. A prolonged pharmacological

blockade of type-5 metabotropic glutamate receptors protects cultured spinal cord motor neurons against excitotoxic death. Neurobiol. Dis. 42, 252-264.

Dingledine, R., Borges, K., Bowie, D., Traynelis, S.F., 1999. The glutamate receptor ion channels. Pharmacol. Rev. 51, 7-61.

Eisen A. 2009. Amyotrophic lateral sclerosis: A 40-year personal perspective. J. Clin. Neurosci. 16, 505-512.

Ferraiuolo, L., Kirby, J., Grierson, A.J., Sendtner, M. and Shaw,P.J. 2011. Molecular pathways of motor neuron injury in amyotrophic lateral sclerosis. Nat. Rev. Neurol. 7, 616-630.

Fleck, M.,W., Barrionuevo, G., Palmer, A.,M., 2001. Synaptosomal and vesicular accumulation of L-glutamate, L-aspartate and D-aspartate. Neurochem Int. 39, 217-225.

Giribaldi, F., Milanese, M., Bonifacino, T., Rossi, P.,I.,A., Di Prisco, S., Pittaluga, A., Tacchetti, C., Puliti, A., Usai, C., Bonanno, G., 2013. Group I metabotropic glutamate autoreceptors induce abnormal glutamate exocytosis in a mouse model of amyotrophic lateral sclerosis. Neuropharmacology 56, 253-263.

Grynkiewicz, G., Poenie, M., Tsien, R.Y., 1985. A new generation of Ca^{2+} indicators with greatly improved fluorescence properties. J. Biol. Chem. 260, 3440-3450.

Gurney, M.,E., Pu, H., Chiu, A.,Y., Dal Canto, M.,C., Polchow, C.,Y., Alexander, D.,D., Caliendo, J., Hentati, A., Kwon, Y.,W., Deng, H.,X., Chen, W., Zhai, P., Sufit, R.,L., Siddique, T., 1994. Motor neuron degeneration in mice that express a human Cu,Zn superoxide dismutase mutation. Science 264, 1772-1775. Erratum in: Science 269(5221), 149.

Ilieva, H., Polymenidou, M., Cleveland, D.,W., 2009. Non-cell autonomous toxicity in neurodegenerative disorders: ALS and beyond. J Cell Biol 187, 761-772.

Jonas, P., and Burnashev, N., 1995. Molecular mechanisms controlling calcium entry through AMPA-type glutamate receptor channels. Neuron 15, 987–990.

Kaur, S.,J., McKeown, S.,R., Rashid, S., 2016. Mutant SOD1 mediated pathogenesis of Amyotrophic Lateral Sclerosis. Gene. 577, 109-118.

Kovàcs, A.,D., and Pearce, D.,A., 2013. Location- and sex-specific differences in weight and motor coordination in two commonly used mouse strains. Sci Rep. 3, 2116-2122.

Lasiene, J., Yamanaka, K., 2011. Glial cells in amyotrophic lateral sclerosis. Neurol. Res. Int. 718987.

Laslo, P., Lipski, J., Funk, G.,D., 2003. Differential expression of Group I metabotropic glutamate receptors in motoneurons at low and high risk for degeneration in ALS. Neuroreport. 12(9), 1903-1908.

Laslo, P., Lipski, J., Nicholson, L.,F., Miles, G.,B., Funk, G.,D., 2001. GluR2 AMPA receptor subunit expression in motoneurons at low and high risk for degeneration in amyotrophic lateral sclerosis. Exp. Neurol. 169, 461–471.

Liu, G.,J., Nagarajah, R., Banati, R.,B., Bennett, M.,R., 2009. Glutamate induces directed chemotaxis of microglia. Eur J Neurosci 29, 1108–1118.

Lu, Y.,M., Jia, Z., Janus, C., Henderson, J.,T., Gerlai, R., Wojtowicz, J.,M., Roder, J.,C., 1997 Mice lacking metabotropic glutamate receptor 5 show impaired learning and reduced CA1 long-term potentiation (LTP) but normal CA3 LTP. J Neurosci. 17, 5196-5205.

McGoldrick, P., Joyce, P.,I., Fisher, E.,M., Greensmith, L., 2013, Rodent models of amyotrophic lateral sclerosis. Biochim Biophys Acta. 1832, 1421-1436.

Meziane, H., Ouagazzal, A., M., Aubert, L., Wietrzych, M., Krezel, W., 2007. Estrous cycle effects on behavior of C57BL/6J and BALB/cByJ female mice: implications for phenotyping strategies. Genes Brain Behav. 6, 192–200.

Milanese, M., Bonifacino, T., Fedele, E., Rebosio, C., Cattaneo, L., Benfenati, F., Usai, C., Bonanno, G., 2015. Exocytosis regulates trafficking of GABA and glycine heterotransporters in spinal cord glutamatergic synapses: A mechanism for the excessive heterotransporter-induced release of glutamate in experimental amyotrophic lateral sclerosis. Neurobiol Dis. 74, 314-324.

Milanese, M., Giribaldi, F., Melone, M., Bonifacino, T., Musante, I., Carminati, E., Rossi, P.,I.,A., Vergani, L., Voci, A., Conti, F., Puliti, A., Bonanno, G., 2014. Knocking-down metabotropic glutamate receptor 1 improves survival and disease progression in the SOD1G93A mouse model of amyotrophic lateral sclerosis. Neurobiol. Dis. 64, 48-59.

Milanese, M., Zappettini, S., Jacchetti, E., Bonifacino, T., Cervetto, C., Usai, C., Bonanno, G., 2010. In-vitro activation of GAT1 transporters expressed in spinal cord gliosomes stimulates glutamate release that is abnormally elevated in the SOD1/G93A(+) mouse model of amyotrophioc lateral sclerosis. J. Neurochem. 113, 489-501.

Milanese, M., Zappettini, S., Onofri, F., Musazzi, L., Tardito, D., Bonifacino, T., Messa, M., Racagni, G., Usai, C., Benfenati, F., Popoli, P., Bonanno, G., 2011. Abnormal exocytotic release of glutamate in a mouse model of amyotrophic lateral sclerosis. J Neurochem. 116, 1028-1042.

Naie, K. and Manahan-Vaughan, D., 2004. Regulation by metabotropic glutamate receptor 5 of LTP in the dentate gyrus of freely moving rats: relevance for learning and memory formation. Cereb. Cortex 14, 189–198.

Nakao, H., Nakao, K., Kano, M., Aiba, A. 2007. Metabotropic glutamate receptor subtype-1 is essential for motor coordination in the adult cerebellum. Neurosci Res, 57, 538-543.

Nicoletti, F., Bockaert, J., Collingridge, G.L., Conn, P.J., Ferraguti, F., Schoepp, D.D., Wroblewski, J.T., Pin, J.P., 2011. Metabotropic glutamate receptors: from the workbench to the bedside. Neuropharmacology 60, 1017-1041.

Pasinelli, P. and Brown, R.,H., 2006. Molecular biology of amyotrophic lateral sclerosis: insights from genetics. Nature Reviews Neuroscience 7, 710-723.

Peters, O.,M., Ghasemi, M., Brown, R.,H.,Jr., 2015. Emerging mechanisms of molecular pathology in ALS. J. Clin. Invest. 125, 2548.

Philips, T. and Rothstein, J.,D., 2016. Rodent Models of Amyotrophic Lateral Sclerosis. Curr. Protoc. Pharmacol. 69, 1-21.

Pin, J.,P. and Duvoisin, R., 1995. The metabotropic glutamate receptors: structure and functions. Neuropharmacology 34, 1-26.

Pinteaux-Jones, F., Sevastou, I.,G., Fry, V.,A., Heales, S., Baker, D., Pocock, J.,M., 2008. Myelin-induced microglial neurotoxicity can be controlled by microglial metabotropic glutamate receptors. J Neurochem 106, 442–454.

Raiteri, L., Paolucci, E., Prisco, S., Raiteri, M., Bonanno, G., 2003. Activation of a glycine transporter on spinal cord neurons causes enhanced glutamate release in a mouse model of amyotrophic lateral sclerosis. Br. J. Pharmacol. 138, 1021-1025.

Raiteri, L., Stigliani, S., Zappettini, S., Mercuri, N.,B., Raiteri, M., Bonanno, G., 2004. Excessive and precocious glutamate release in a mouse model of amyotrophic lateral sclerosis. Neuropharmacology 46, 782-792.

Raiteri, L., Zappettini, S., Milanese, M., Fedele, E., Raiteri, M. Bonanno, G., 2007 Mechanisms of glutamate release elicited in rat cerebrocortical nerve endings by 'pathologically' elevated extraterminal K+ concentrations. J. Neurochem. 103: 952–961.

Rosen, D.,R., Siddique, T., Patterson, D., Figlewicz, D.A., Sapp, P., Hentati, A., Donaldson, D., Goto, J., O'Regan, J.P., Deng, H.X. et al., 1993. Mutations in Cu/Zn superoxide dismutase. Nature, 362(6415), 59-62.

Rossi, D., Brambilla, L., Valori, C.,F., Roncoroni, C., Prugnola, A., Yokota, T., Bredesen, D.,E., Volterra, A., 2008. Focal degeneration of astrocytes in amyotrophic lateral sclerosis. Cell. Death. Differ. 15, 1691-1700.

Rossi, P.,I.,A., Musante, I., Summa, M., Pittaluga, A., Emionite, L., Ikehata, M., Rastaldi, M.,P., Ravazzolo, R., Puliti, A., 2013. Compensatory molecular and functional mechanisms in nervous system of the Grm1(crv4) mouse lacking the mGlu1 receptor: a model for motor coordination deficits. Cereb. Cortex 23(9), 2179-2189.

Rothstein, J.,D., Van Kammen, M., Levey, A.,I., Martin, L.,J., Kuncl, R.,W., 1995. Selective loss of glial glutamate transporter GLT-1 in amyotrophic lateral sclerosis. Ann. Neurol. 38, 73-84.

Rothstein, J.,D., Patel, S., Regan, M.,R., Haenggeli, C., Huang, Y.,H., Bergles, D.,E., Jin, L., Dykes Hoberg, M., Vidensky, S., Chung, D.,S., Toan, S.,V., Bruijn, L.,I., Su, Z.,Z., Gupta, P., Fisher, P.,B., 2005. Beta-lactam antibiotics offer neuroprotection by increasing glutamate transporter expression. Nature 433, 73-77.

Shaw P.J., Forrest, V., Ince, P.,G., Richardson, J.,P., Wastell, H.,J., 1995. CSF and plasma amino acid levels in motor neuron disease: elevation of CSF glutamate in a subset of patients. Neurodegeneration. 4, 209-216.

Shaw, P.,J., Williams, T.,L., Slade, J.,Y., Eggett, C.,J., Ince, P.,G., 1999. Low expression of GluR2 AMPA receptor subunit protein by human motor neurons. Neuroreport 10, 261–265.

Siklós, L., Engelhardt, J.,I., Alexianu, M.,E., Gurney, M.,E., Siddique, T., Appel, S.,H., 1998. Intracellular calcium parallels motoneuron degeneration in SOD-1 mutant mice. J. Neuropathol. Exp. Neurol. 57(6), 571-587.

Siklós, L., Engelhardt, J., Harati, Y., Smith, R.,G., Joó, F., Appel, S.,H., 1996. Ultrastructural evidence for altered calcium in motor nerve terminals in amyotropic lateral sclerosis. Ann. Neurol. 39(2), 203-216.

Simon, N.,G., Turner, M.,R., Vucic, S., Al-Chalabi, A., Shefner, J., Lomen-Hoerth, C., Kiernan, M.,C., 2014. Quantifying disease progression in amyotrophic lateral sclerosis. Ann. Neurol. 76, 643-657.

Simonyi, A., Schachtman, T.,R., Christoffersen, G.,R., 2005. The role of metabotropic glutamate receptor 5 in learning and memory processes. Drug News Perspect. 18(6), 353-361.

Spalloni, A., Albo, F., Ferrari, F., Mercuri, N., Bernardi, G., Zona, C., Longone, P., 2004. Cu/Zn-superoxide dismutase (GLY93ALA) mutation alters AMPA receptor subunit expression and function and potentiates kainate-mediated toxicity in motor neurons in culture. Neurobiol. Dis. 15, 340–350.

Stifanese, R., Averna, M., De Tullio, R., Pedrazzi, M., Beccaria, F., Salamino, F., Milanese, M., Bonanno, G., Pontremoli, S., Melloni, E., 2010. Adaptive modifications in the calpain/calpastatin system in brain cells after persistent alteration in Ca^{2+} homeostasis. J. Biol. Chem. 285, 631-643.

Stifanese, R., Averna, M., De Tullio, R., Pedrazzi, M., Milanese, M., Bonifacino, T., Bonanno, G., Salamino, F., Pontremoli, S., Melloni, E., 2014. Role of calpain-1 in the early phase of experimental ALS. Arch. Biochem. Biophys. 562, 1–8.

Swanson, C.,J. and Kalivas, P.,W., 2000. Regulation of locomotor activity by metabotropic glutamate receptors in the nucleus accumbens and ventral tegmental area. J. Pharmacol Expl Ther 292, 406-414.

Takuma, H., Kwak, S., Yoshizawa, T., Kanazawa, I., 1999. Reduction of GluR2 RNA editing, a molecular change that increases calcium influx through AMPA receptors, selective in the spinal ventral gray of patients with amyotrophic lateral sclerosis. Ann. Neurol. 46, 806–815.

Uccelli, A., Milanese, M., Principato, M.,C., Morando, S., Bonifacino, T., Vergani, L., Giunti, D., Voci, A., Carminati, E., Giribaldi, F., Caponnetto C., Bonanno, G., 2012. Intravenous Mesenchymal Stem Cells Improve Survival and Motor Function in Experimental Amyotrophic Lateral Sclerosis. Mol. Med. 18, 794-804.

Urbani, A., Belluzzi, O., 2000. Riluzole inhibits the persistent sodium current in mammalian CNS neurons. Eur. J. Neurosci. 12, 3567-3574.

Vandenberghe, W., Robberecht, W., Brorson, J.,R., 2000. AMPA receptor calcium permeability, GluR2 expression, and selective motoneuron vulnerability. J Neurosci., 20, 123–132.

Valerio, A., Ferrario, M., Paterlini, M., Liberini, P., Moretto, G., Cairns, N.,J., Pizzi, M., Spano, P., 2002. Spinal cord mGlu1a receptors: possible target for amyotrophic lateral sclerosis therapy. Pharmacol. Biochem. Behav. 73, 447-454.

Van Den Bosch, L, Vandenberghe, W., Klaassen, H., Van Houtte, E., Robberecht, W., 2000. Ca^{2+}-permeable AMPA receptors and selective vulnerability of motor neurons. J. Neurol. Sci. 180, 29–34.

Wuolikainen, A., Moritz, T., Marklund, S.,L., Antti, H., Andersen, P.,M., 2011. Disease-related changes in the cerebrospinal fluid metabolome in amyotrophic lateral sclerosis detected by GC/TOFMS. PLoS One 6, e17947.

Zona, C., Siniscalchi, A., Mercuri, N.B., Bernardi, G., 1998. Riluzole interacts with voltage-activated sodium and potassium currents in cultured rat cortical neurons. Neuroscience 85, 931-938.

LEGENDS TO THE FIGURES

Figure 1. Schematic representation of animal crossing. *SOD1*^{G93A} male mice were bred with *Grm5*$^{-/+}$ females to generate four genetically distinct mouse littermates (WT, *Grm5*$^{-/+}$, *SOD1*^{G93A} and *SOD1*^{G93A}*Grm5*$^{-/+}$) being the *SOD1*^{G93A}*Grm5*$^{-/+}$ a double-mutants mouse carrying the *Grm5*$^{-/+}$ heterozygous mutation and the SOD1*G93A transgene. All experiments were conducted on littermates derived from F1 crossing.

Figure 2. mGluR1 and mGluR5 expression. Expression of mGluR1 and mGluR5 in *SOD1*^{G93A} or *SOD1*^{G93A}*Grm5*$^{-/+}$ mice (**A**) and in WT and *Grm5*$^{-/+}$ mice (**B**) is reported. mGluR1 and mGluR5 proteins were determined in lumbar spinal cord homogenates by SDS-PAGE and Western blotting using a mouse anti-mGluR1 monoclonal antibody or a rabbit anti-mGluR5 polyclonal antibody. Representative immunoreactive bands are reported above the respective quantification graph. Data are Means ± s.e.m of 6 independent experiments (6 mice per group; 3 females and 3 males). *$p < 0.01$ (Student't t-test).

Figure 3. Survival. Survival probability was determined by Kaplan-Meier analysis in mixed sex (**A**), female (**B**) and male (**C**) *SOD1*^{G93A}*Grm5*$^{-/+}$ and *SOD1*^{G93A} mice . Survival time was assumed as the time when animals were unable to right itself within 20 s when placed on their side. 21 female and 25 male *SOD1*^{G93A}*Grm5*$^{-/+}$ mice and 18 female and 21 male *SOD1*^{G93A} mice were analysed. Survival probability was significantly augmented in mixed sex *SOD1*^{G93A}*Grm5*$^{-/+}$ compared to *SOD1*^{G93A} mice (p<0.001) as well as in female (p<0.001) and male (p<0.001) *SOD1*^{G93A}*Grm5*$^{-/+\ mice}$ (Log-rank test).

Figure 4. Body weight. Body weight was measured immediately before behavioural tests in female (**A**) or male (**B**) WT, *SOD1*^{G93A}, and *SOD1*^{G93A}*Grm5*$^{-/+}$ mice. Sexes were studied separately for the obvious constitutive weight differences. 10 female and 10 male WT mice; 21 female and 25 male *SOD1*^{G93A}*Grm5*$^{-/+}$ mice and 18 female and 21 male *SOD1*^{G93A} mice were used. Data reported are means ± s.e.m. *$p < 0.05$ at least vs. WT (Mann–Whitney Rank Sum Test). Vertical dotted lines indicate the time of the first significant difference vs. WT mice.

Figure 5. Rotarod. The time of permanence on the rotating bar of the Rotarod apparatus was used to determine the disease progression in in mixed sex (**A**), female (**B**) and male (**C**) *SOD1*^{G93A}*Grm5*$^{-/+}$ and *SOD1*^{G93A} mice. Animals were tested three days a week starting on day 90. Falling off time was recorded. 18 female and 15 male *SOD1*^{G93A}*Grm5*$^{-/+}$ mice and 15 female and 13 male *SOD1*^{G93A} mice were analysed. Data reported are means ± s.e.m. The Rotarod performance was significantly augmented in male *SOD1*^{G93A}*Grm5*$^{-/+}$vs. *SOD1*^{G93A} mice (*$p < 0.05$ at least) (Mann–Whitney Rank Sum Test). No significant differences were observed in mixed sex and in female *SOD1*^{G93A}*Grm5*$^{-/+}$ mice.

Figure 6. Extension reflex. Hind limb extension reflex was used to determine the disease progression in mixed sex (**A**), female (**B**) and male (**C**) *SOD1*^{G93A}*Grm5*$^{-/+}$ and *SOD1*^{G93A} mice. Animals were tested three days a week starting on day 90. Animals were rated according to a 5-0 score scale. 18 female and 15 male *SOD1*^{G93A}*Grm5*$^{-/+}$ mice and 15 female and 13 male *SOD1*^{G93A} mice were analysed. Data reported are means ± s.e.m. The extension reflex score was significantly augmented in male *SOD1*^{G93A}*Grm5*$^{-/+}$ vs. *SOD1*^{G93A} mice (*$p < 0.05$ at least) (Mann–Whitney Rank Sum Test). No significant differences were observed in mixed sex and in female

SOD1^{G93A}*Grm5*$^{-/+}$ mice.

Figure 7. Gait. Gait impairment in an open field was used to determine the disease progression in in mixed sex (**A**), female (**B**) and male (**C**) *SOD1*^{G93A}*Grm5*$^{-/+}$ and *SOD1*^{G93A} mice. Animals were tested three days a week starting on day 90. Animals were rated according to a 5-0 score scale. 18 female and 15 male *SOD1*^{G93A}*Grm5*$^{-/+}$ mice and 15 female and 13 male *SOD1*^{G93A} mice were analysed. Data reported are means ± s.e.m. The gait score was significantly augmented in male *SOD1*^{G93A}*Grm5*$^{-/+}$ vs. *SOD1*^{G93A} mice (*$p < 0.05$ at least) (Mann–Whitney Rank Sum Test). No significant differences were observed in mixed sex and in female *SOD1*^{G93A}*Grm5*$^{-/+}$ mice.

Figure 8. Motor neuron number. The number of spinal motor neurons in the vetrolateral horn was determined in WT, *SOD1*^{G93A}, *Grm5*$^{-/+}$, and *SOD1*^{G93A}*Grm5*$^{-/+}$ mouse L4/L5 lumbar spinal cord sections. Representative photomicrograph (scale bar 100 µm). (**A**) and motor neuron quantification (**B**) are reported Mice were anesthetized and perfused transcardially with paraformaldehyde. Spinal cords were post-fixed and stored at -20°C. Sections (50 µm-thick) were stained with thionine. Alpha-motoneurons were selected and counted based on diameters greater than 25 µm. Data are means ± s.e.m. of 20 sections from 3 mice per group (2 female and 1 male WT; 1 female and 2 male *SOD1*^{G93A}; 1female and 2 male *Grm5*$^{-/+}$ and 1 female and 2 male *SOD1*^{G93A}*Grm5*$^{-/+}$). *$p < 0.01$ vs. WT; $^{\#}p < 0.01$ vs. *SOD1*^{G93A} (One-way ANOVA and Bonferroni post-hoc tests).

Figure 9. Astrogliosis and microgliosis. The expression of GFAP and CD11β was measured as index of astrogliosis and activated microglia, respectively, in WT, *SOD1*^{G93A}, *SOD1*^{G93A}*Grm5*$^{-/+}$, and *Grm5*$^{-/+}$ mouse spinal cord homogenates.

Representative blots (**A**), astrogliosis (**B**) and activated microglia quantification (**C**) are reported. GFAP and CD11β were determined by SDS-PAGE and Western blotting using a mouse anti-GFAP monoclonal antibody and a rabbit anti-CD11β monoclonal antibody. Data are means ± s.e.m of 4 independent experiments (4 mice per group; 1 female and 3 male WT; 2 female and 2 male *SOD1*^{G93A}; 3 female and 1 male *Grm5*$^{-/+}$ and 2 female and 2 male *SOD1*^{G93A}*Grm5*$^{-/+}$) run in triplicate. **p*<0.01 vs. WT; $^{\#}p < 0.05$, vs. *SOD1*^{G93A} (One-way ANOVA and Bonferroni's post-hoc tests).

Figure 10. Cytosolic Ca^{2+} concentration. $[Ca^{2+}]_C$ was measured in WT, *SOD1*^{G93A}, *Grm5*$^{-/+}$, and *SOD1*^{G93A}*Grm5*$^{-/+}$ mouse spinal cord synaptosomes. Basal (**A**), 3,5-DHPG-evoked (**B**) or KCl-evoked (**C**) $[Ca^{2+}]_C$ are reported. Synaptosomes were labelled with FURA 2-AM and exposed to standard medium or 0.3 and 30 μM 3,5-DHPG or 25 mM KCl. $[Ca^{2+}]_C$ was determined fluorometrically by alternating the excitation wavelengths of 340 and 380 nm. Fluorescent emission was monitored at 510 nm. Results are expressed as nM Ca^{2+}. Data are means ± s.e.m. of 4 independent experiments (4 mice per group; 2 female and 2 male WT; 2 female and 2 male *SOD1*^{G93A}; 3 female and 1 male *Grm5*$^{-/+}$ and 2 female and 2 male *SOD1*^{G93A}*Grm5*$^{-/+}$) run in triplicate, for each experimental condition. **p*<0.05, ***p*<0.01, ****p*<0.001 compared to WT; $^{\#}p$<0.05 compared to *SOD1*^{G93A} (One-way ANOVA followed by Bonferroni post-hoc tests).

Figure 11. Glutamate release. Release was measured in WT, *SOD1*^{G93A}, *Grm5*$^{-/+}$, and *SOD1*^{G93A}*Grm5*$^{-/+}$ mouse spinal cord synaptosomes. Basal (**A**), 3,5-DHPG-evoked (**B**) or KCl-evoked (**C**) [^{3}H]D-Asp release is reported. Synaptosomes were loaded with [^{3}H]D-Asp, in order to label the intra-terminal releasing pools of Glu, and exposed in superfusion to standard medium, 0.3 and 30 μM 3,5-DHPG or 15 mM KCl. Superfusion

samples were counted for radioactivity. Results are expressed as fractional rate per cent (basal release); per cent increase of basal release (3,5-DHPG) or stimulus-evoked overflow (KCl). Data are means ± s.e.m. of 6 independent experiments (6 mice per group; 3 female and 3 male WT; 3 female and 3 male $SOD1^{G93A}$; 3 female and 3 male $Grm5^{-/+}$ and 3 female and 3 male $SOD1^{G93A}Grm5^{-/+}$ for the basal and the KCl-evoked release experiments), 4 independent experiments (4 mice per group; 3 female and 1 male WT; 2 female and 2 male $SOD1^{G93A}$; 3 female and 1 male $Grm5^{-/+}$ and 1 female and 3 male $SOD1^{G93A}Grm5^{-/+}$ for the 3,5-DHPG-evoked release experiments) run in triplicate. *$p < 0.05$, **$p < 0.01$, compared to WT; $^{\#}p < 0.05$ compared to $SOD1^{G93A}$; §$p < 0.01$ §§$p < 0.001$ vs. the respective control (One-way or two-way ANOVA followed by Bonferroni post-hoc tests).

Figure 1
Click here to download high resolution image

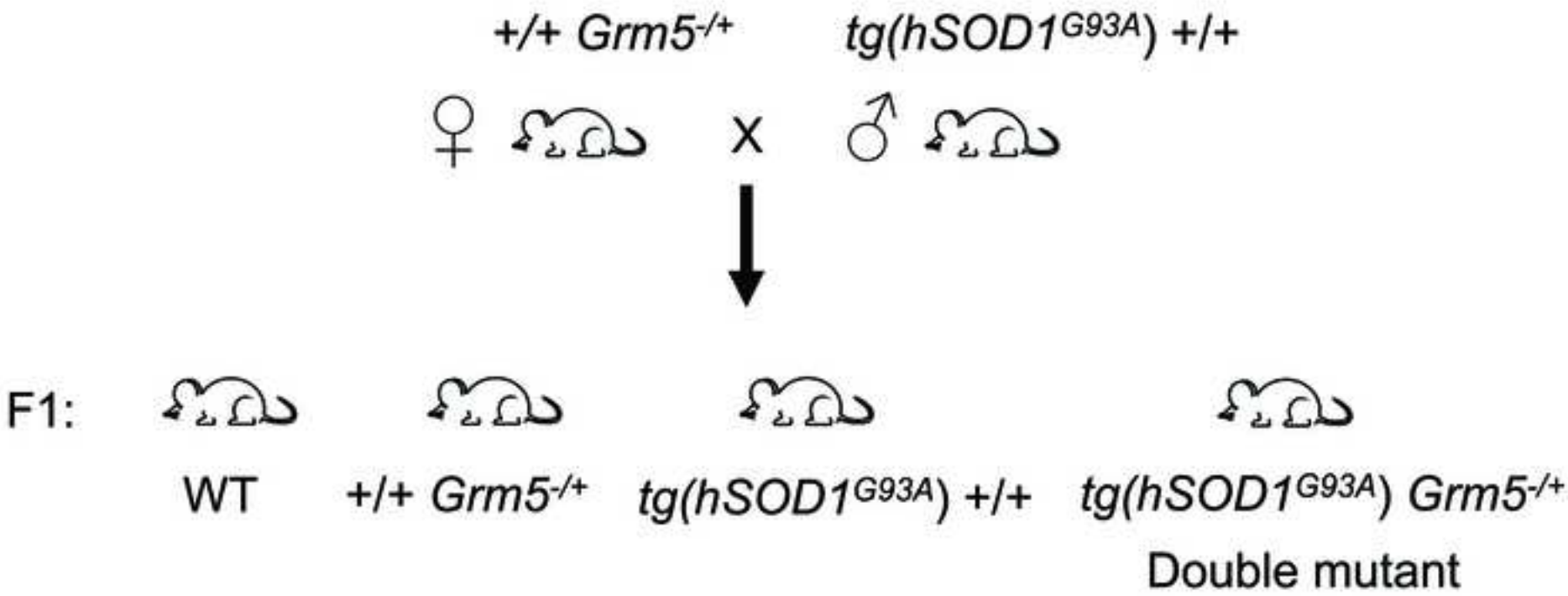

Figure 1

Figure 2
Click here to download high resolution image

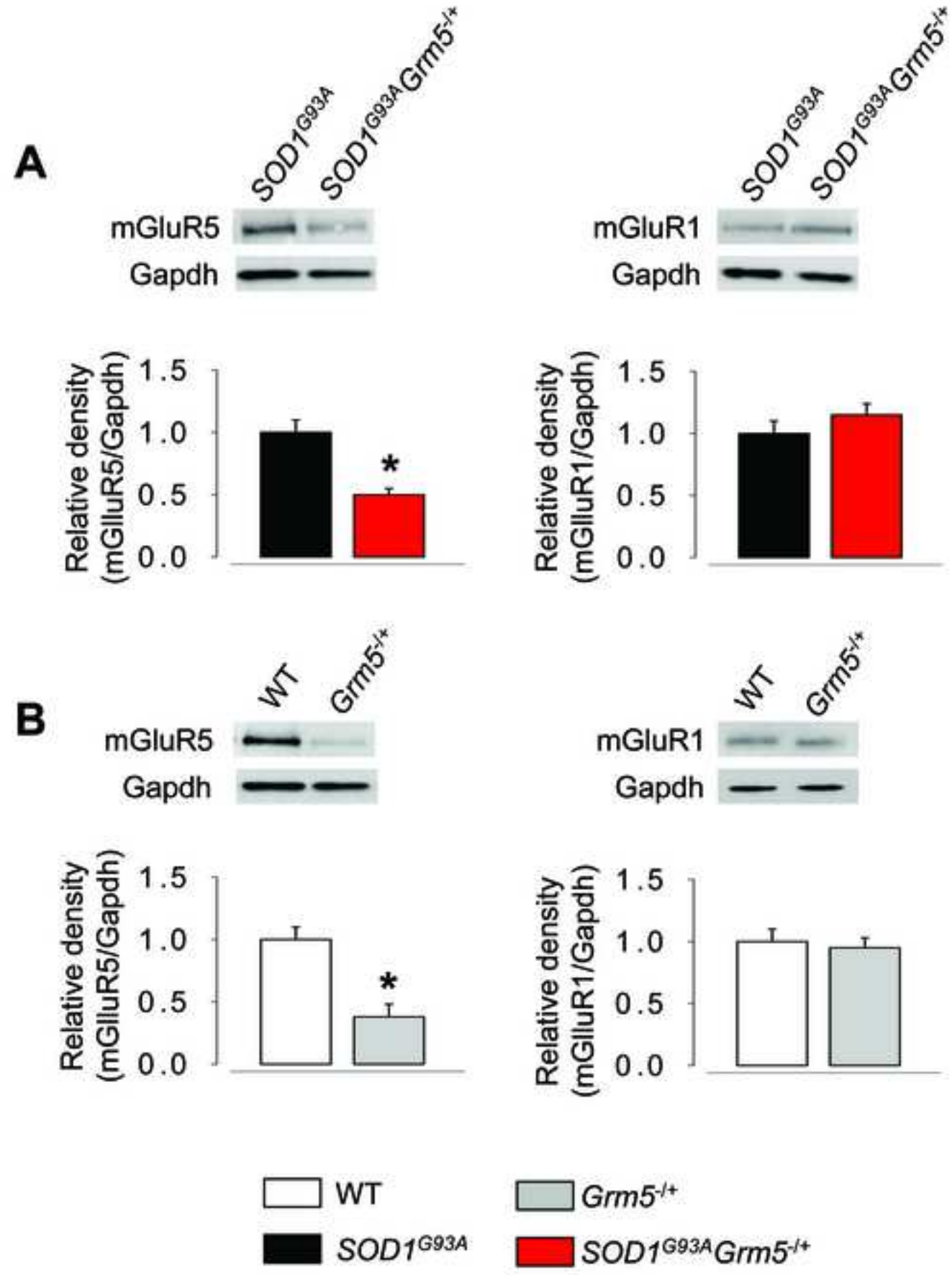

Figure 2

Figure 3
Click here to download high resolution image

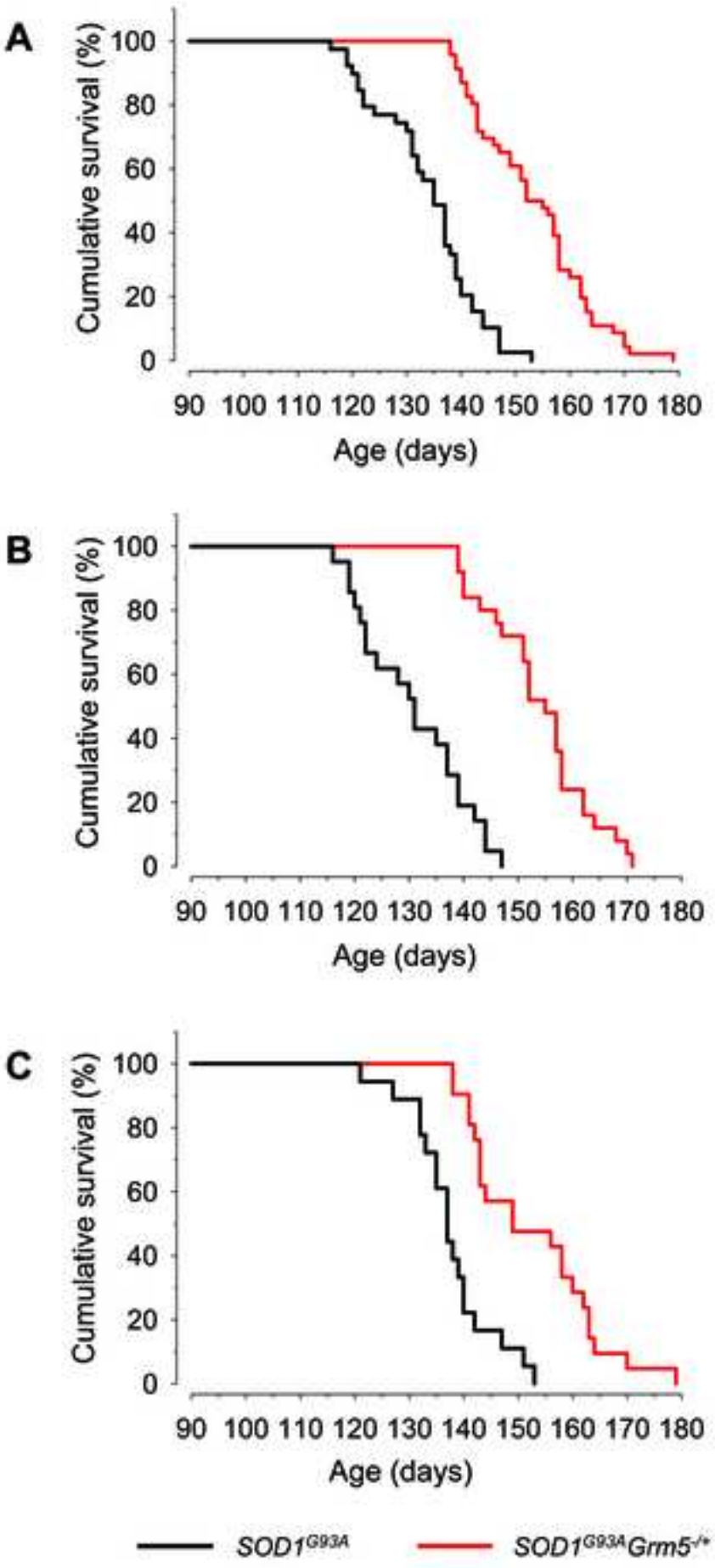

Figure 3

Figure 4
Click here to download high resolution image

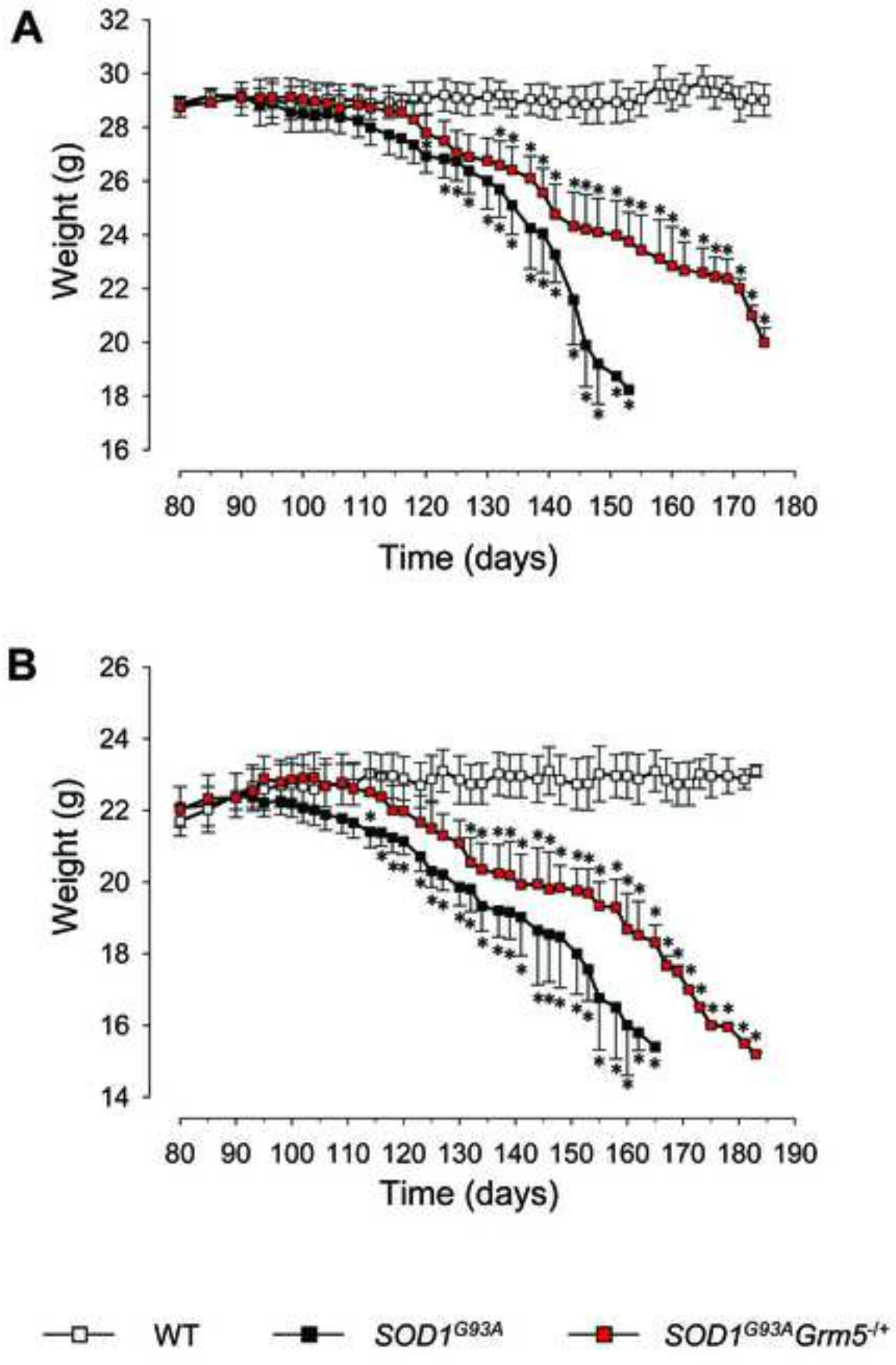

Fugure 4

Figure 5

Click here to download high resolution image

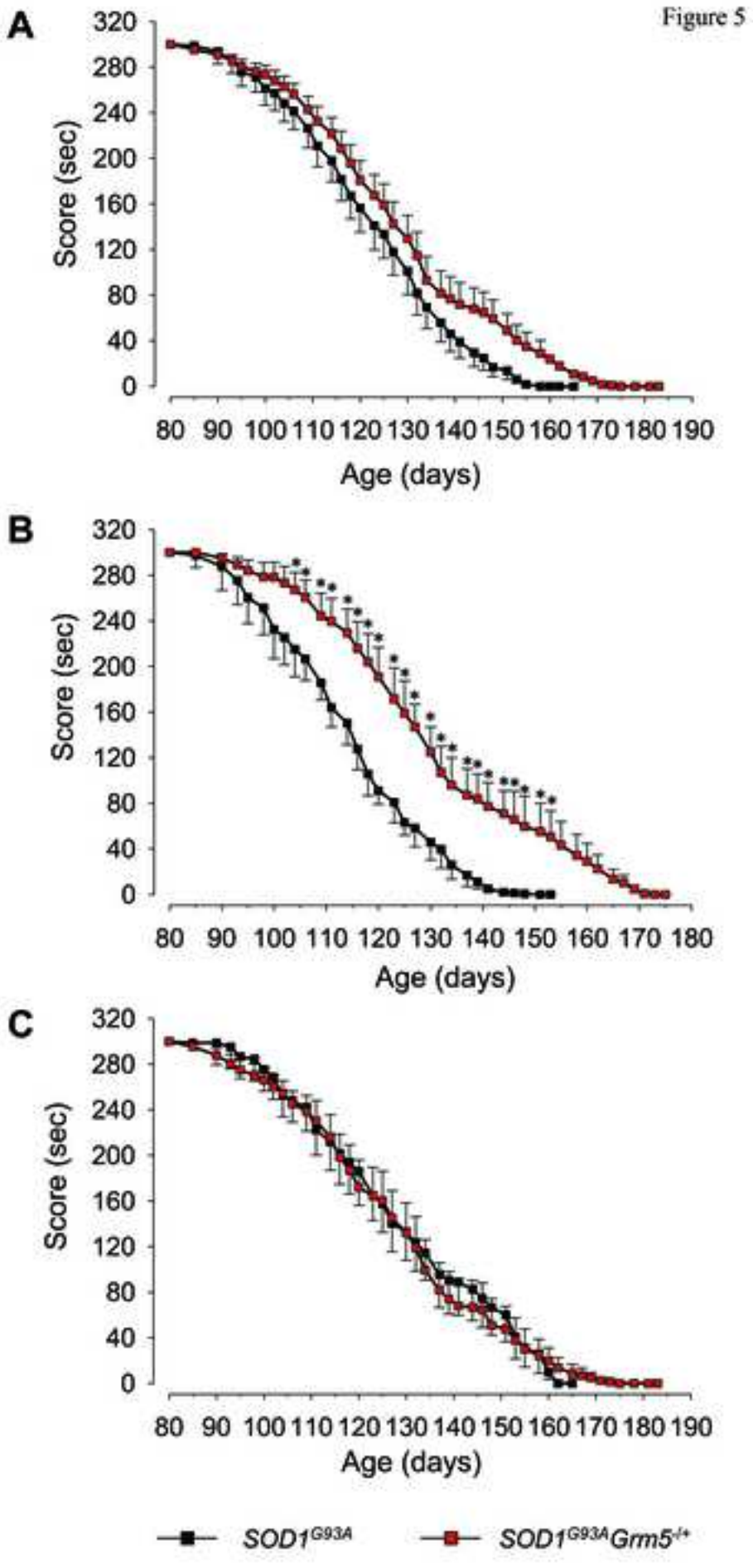

Figure 6

Click here to download high resolution image

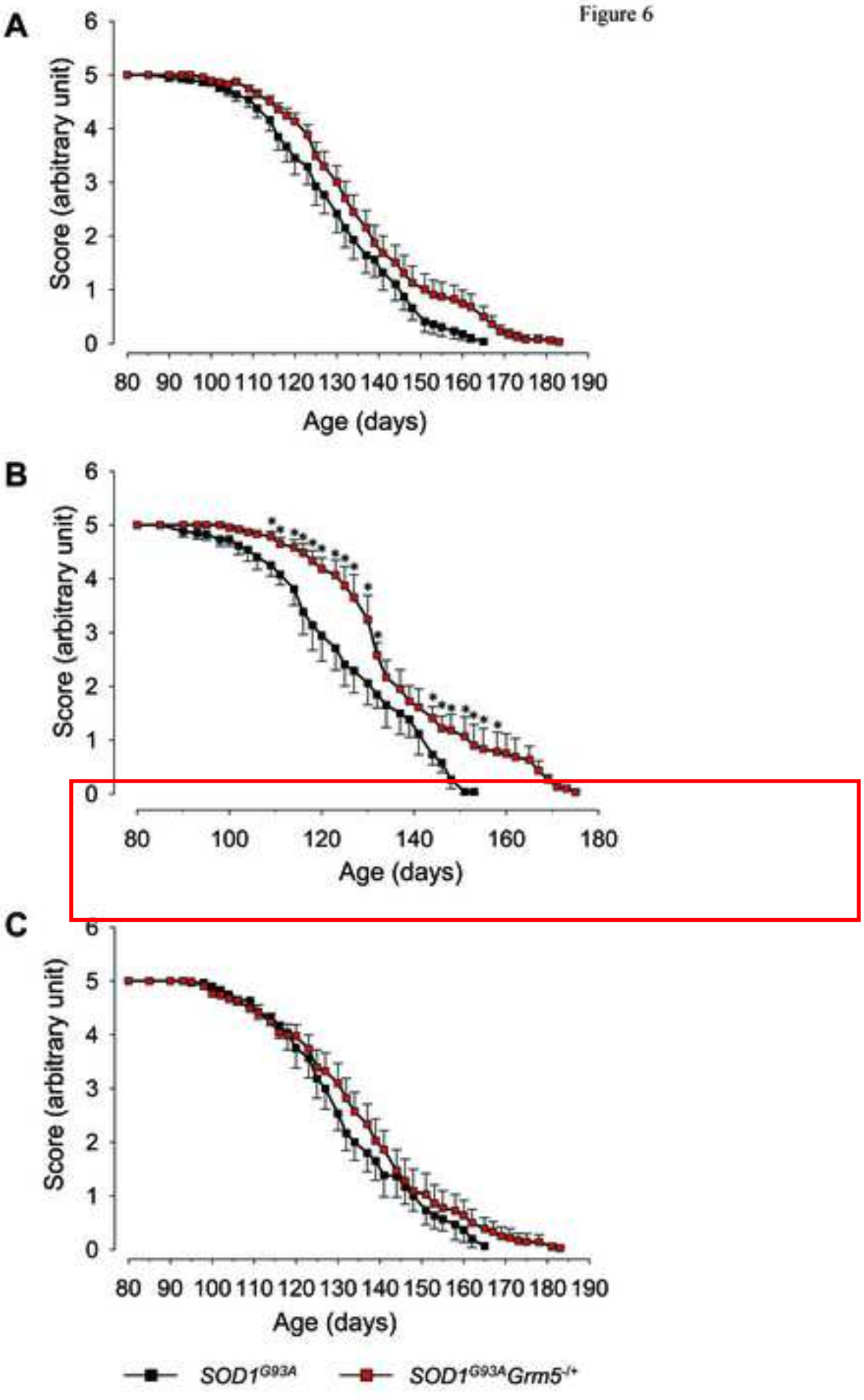

Figure 7

Click here to download high resolution image

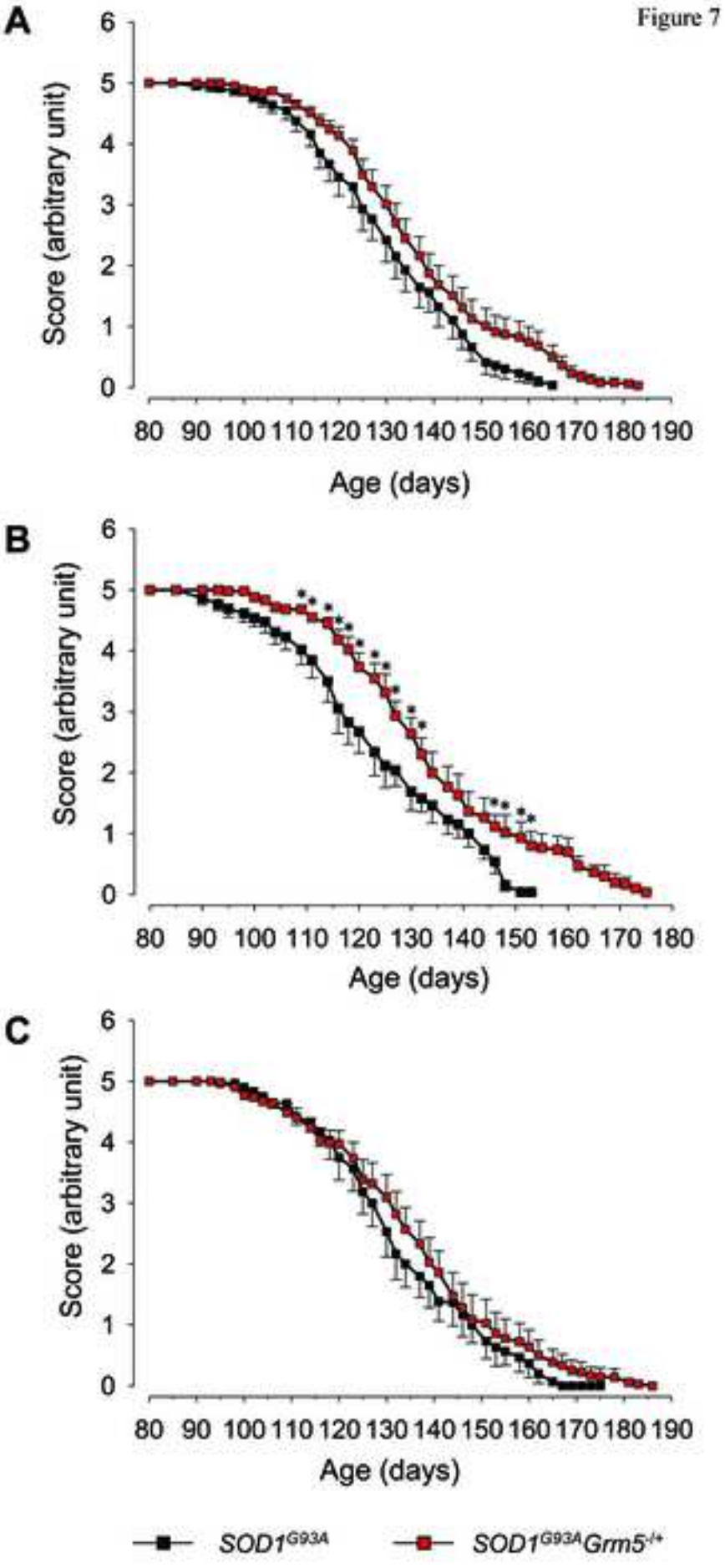

Figure 8
Click here to download high resolution image

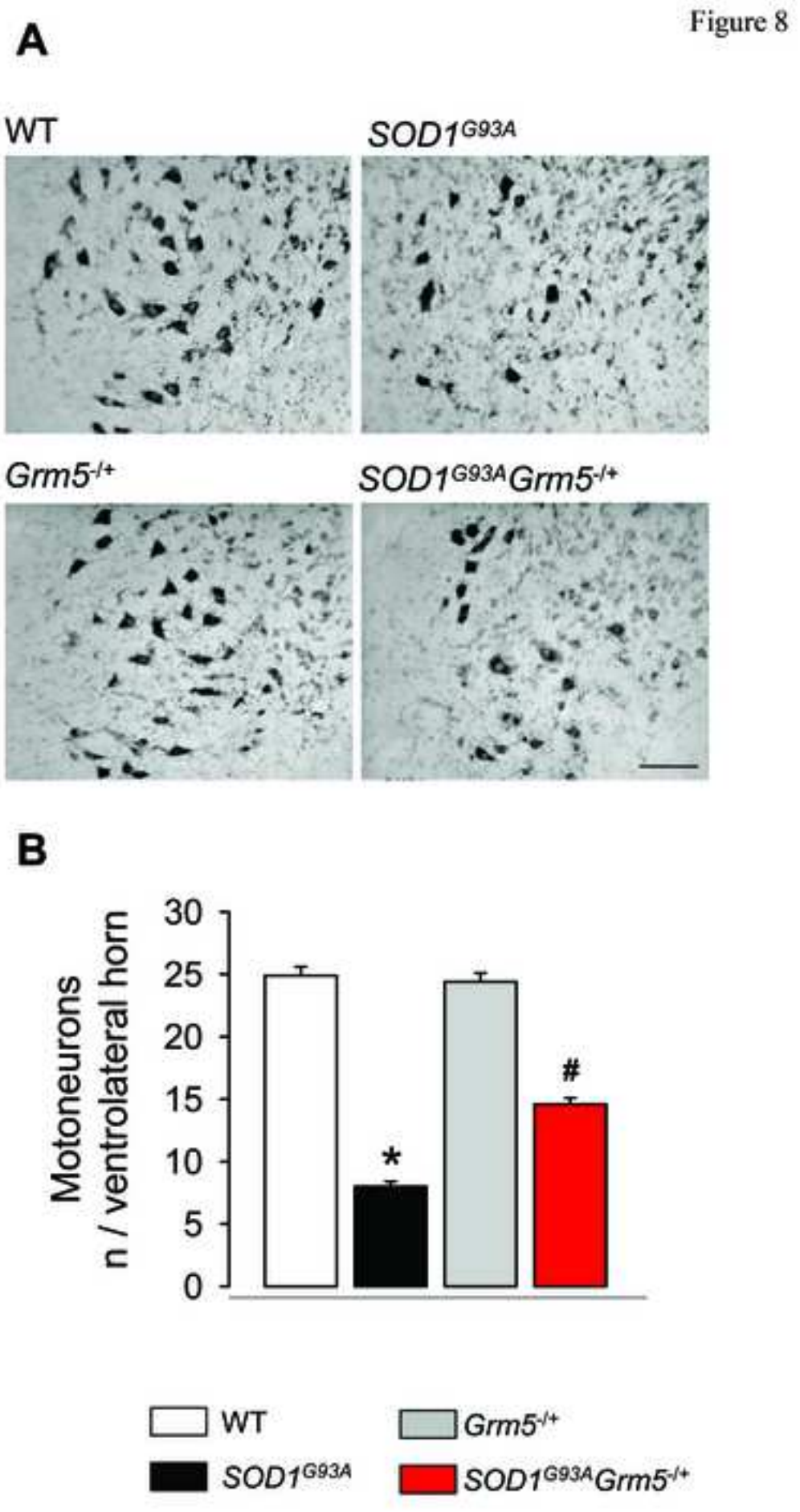

Figure 9
Click here to download high resolution image

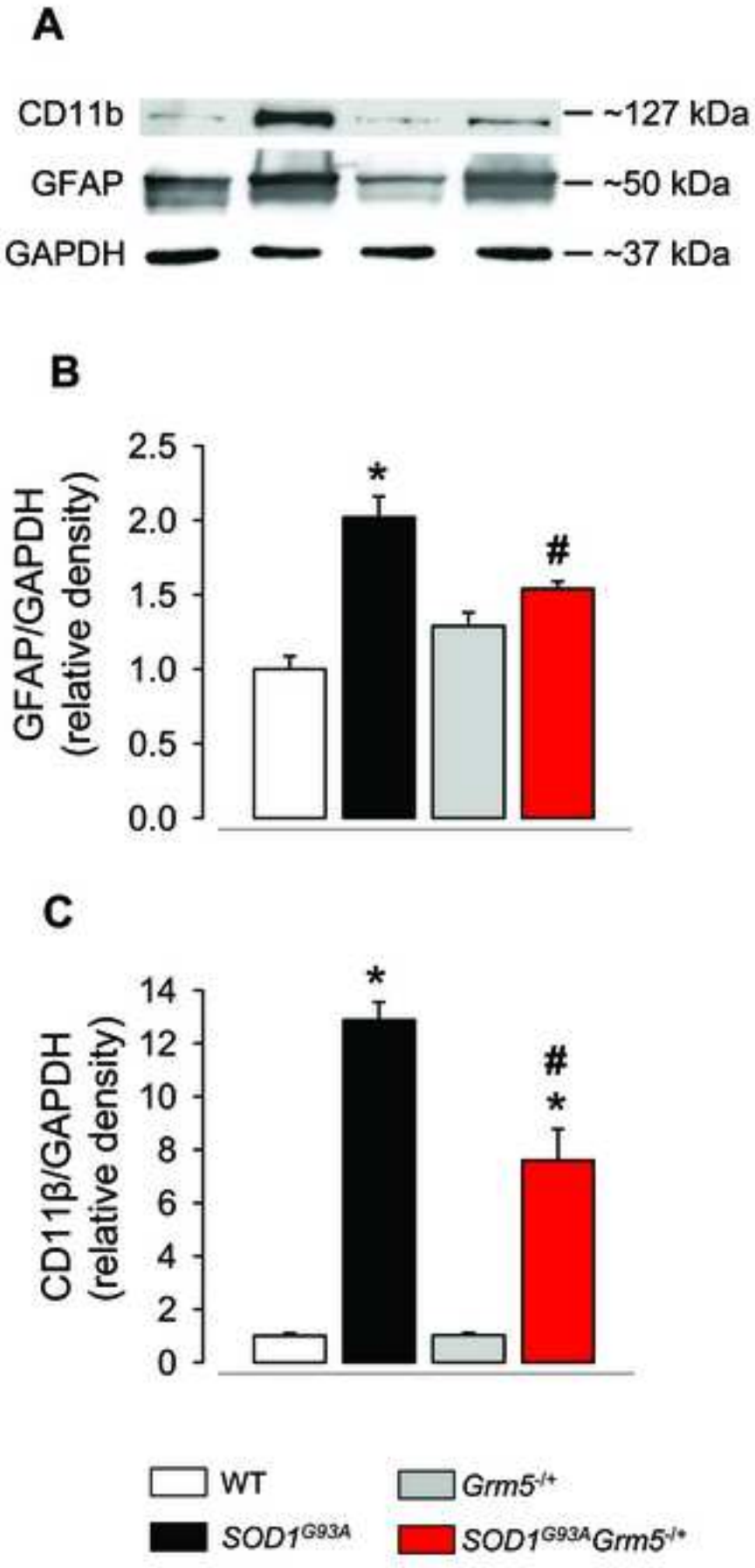

Figure 9

Figure 10
Click here to download high resolution image

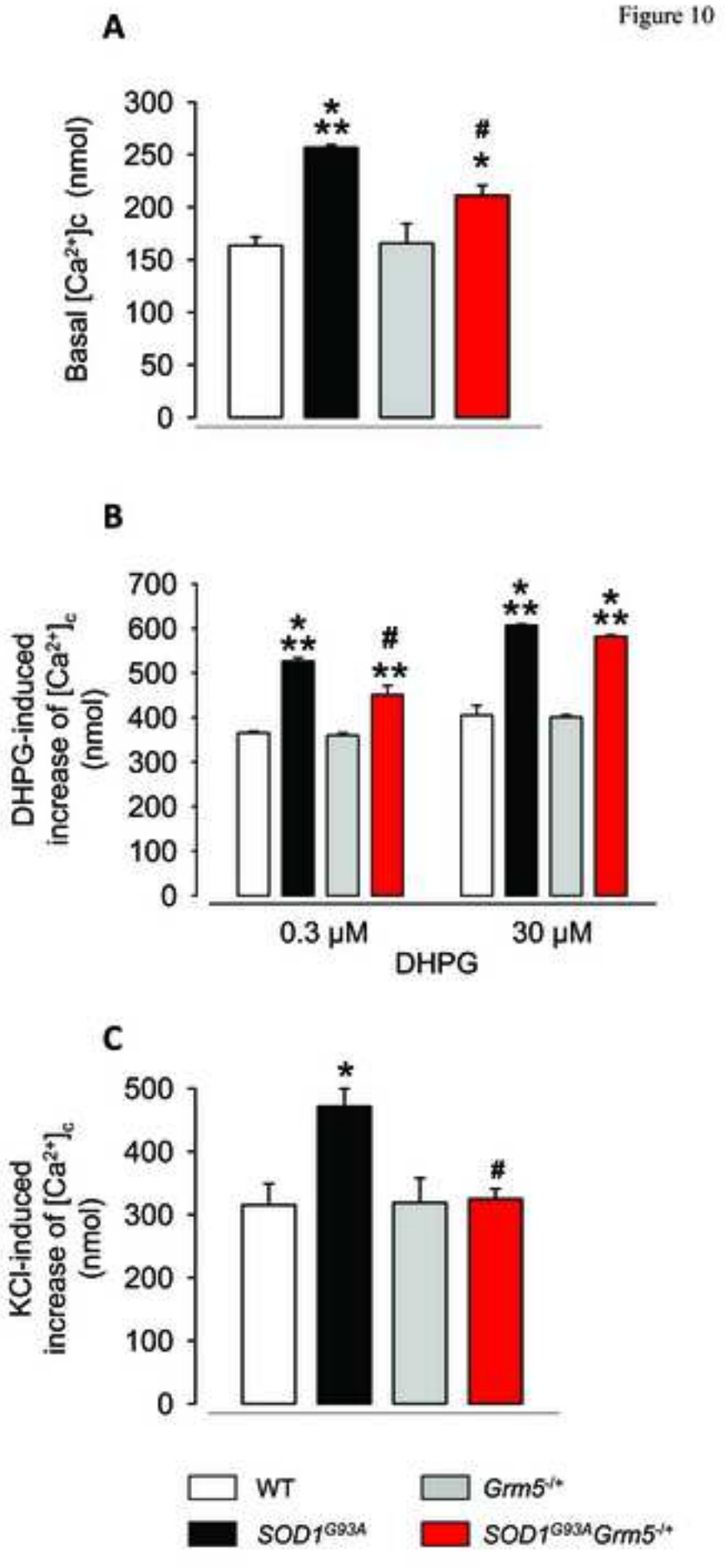

Figure 11
Click here to download high resolution image